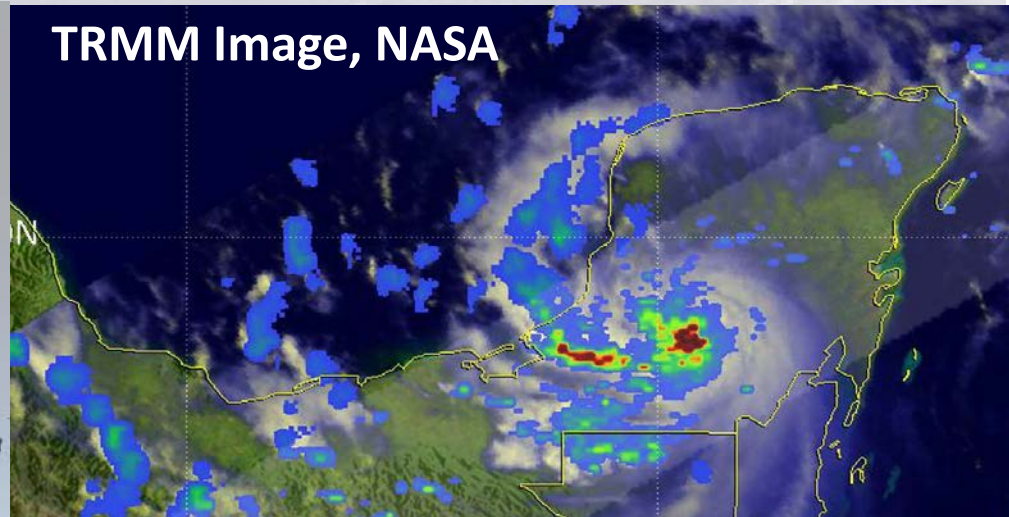


A Study on Airborne GPS Radio Occultations (ROs) and their Impact on Hurricane Karl (2010) Forecast

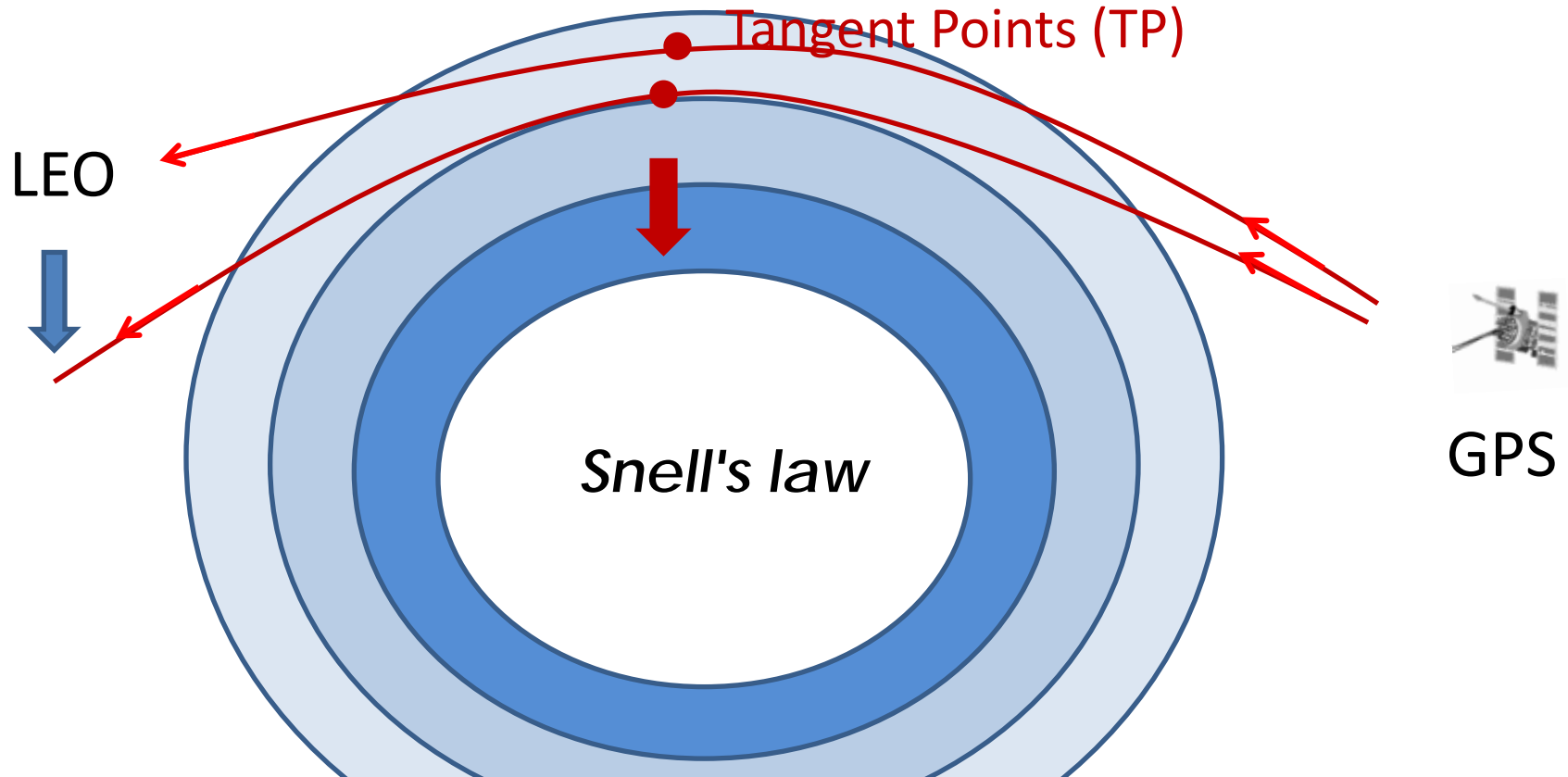
Shu-Hua Chen

University of California, Davis, CA

and X. M. Chen, J. S. Haase, B. J. Murphy, K. N. Wang,
J. L. Garrison, L. Adhikari, F. Xie, S. Y. Chen, C. Y. Huang

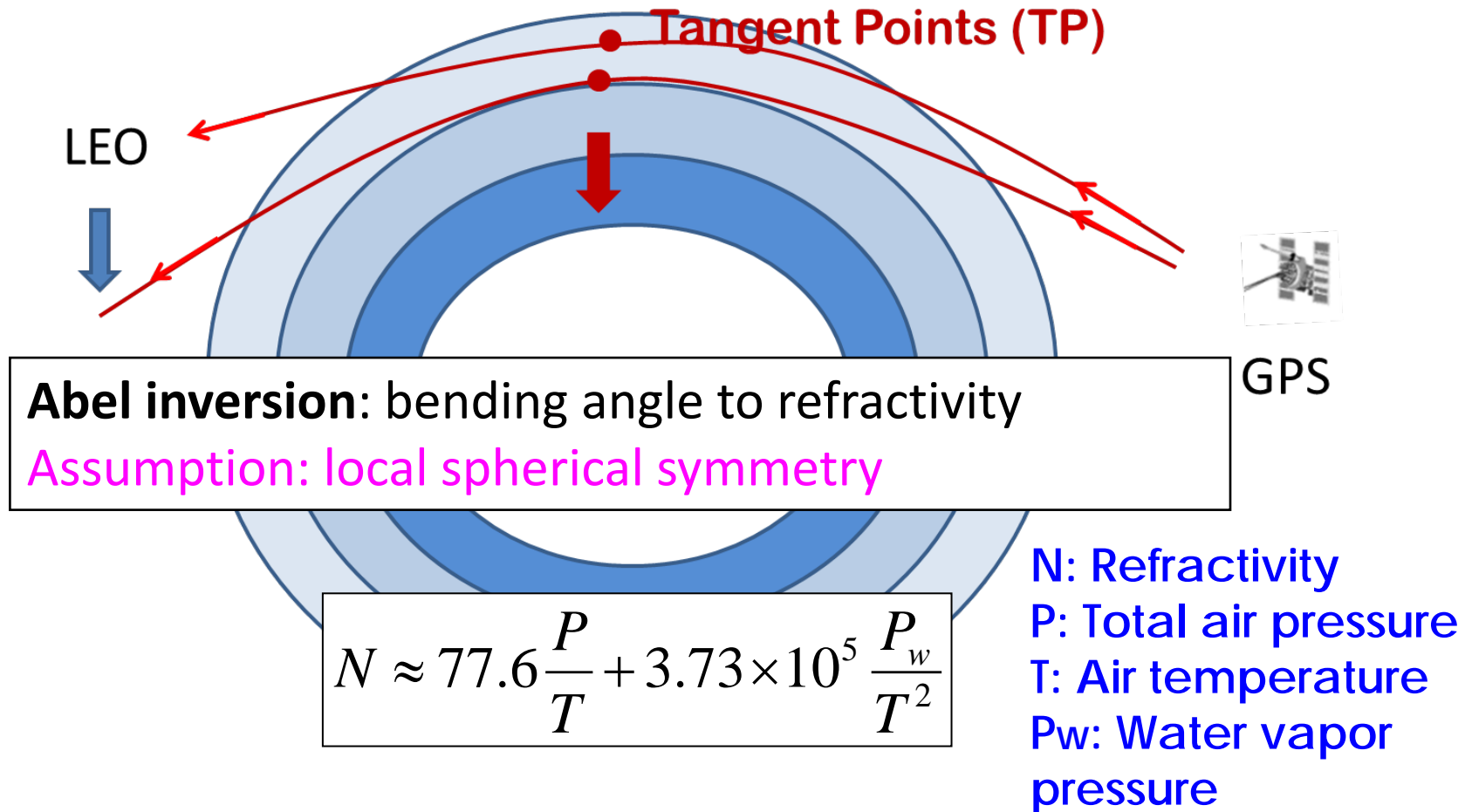


Spaceborne GPS Radio Occultation (RO)



- GPS RO measurements are nearly weather free !
- Have a great vertical resolution !

Refractivity

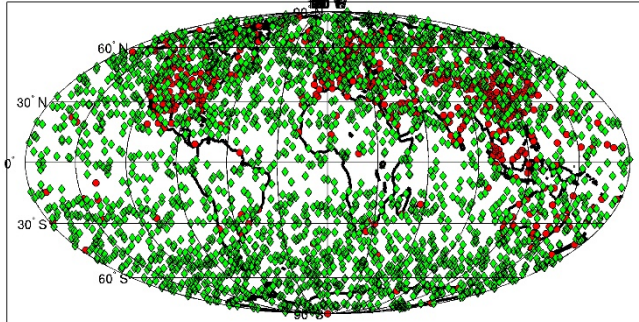


Observable = phase data → Doppler shift
→ bending angle → refractivity

The RO data provide temperature, moisture, and pressure information.

COSMIC 2006

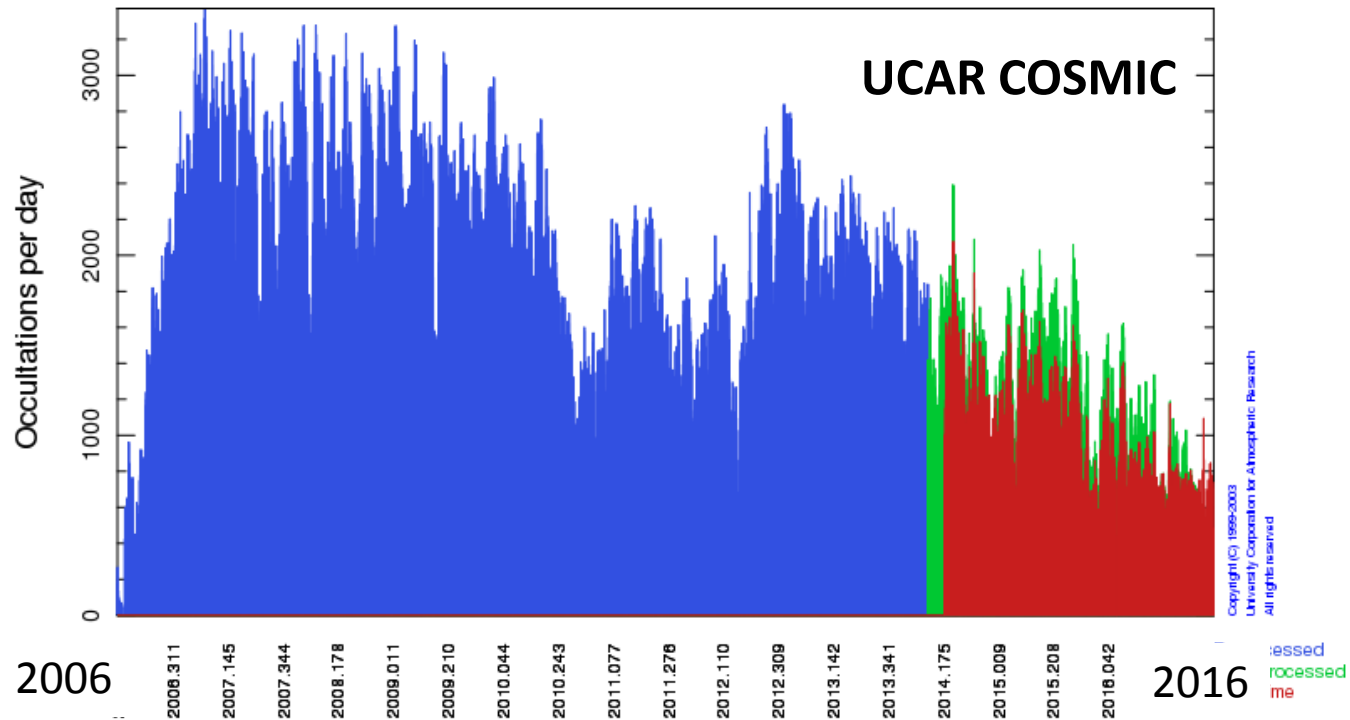
Occultation Locations for COSMIC, 6 S/C, 6 Planes, 24 Hrs



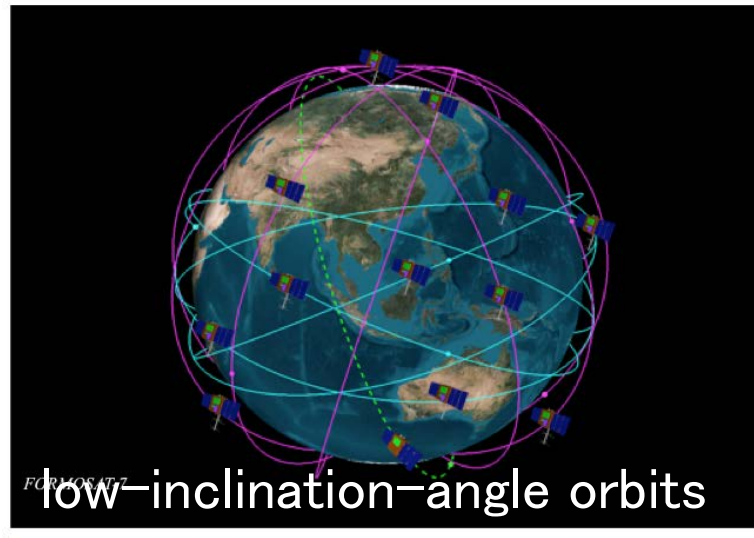
- Radiosonde locations
- ◆ Occultation locations

Processed data for cosmic: 2006.111-2017.057

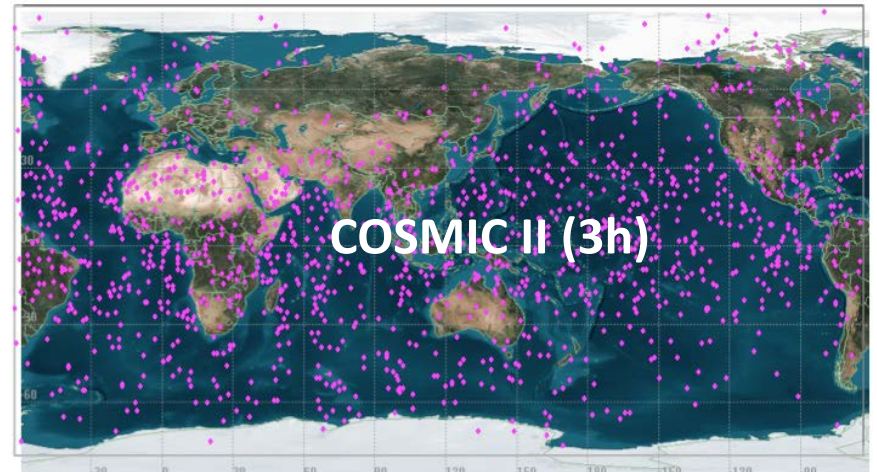
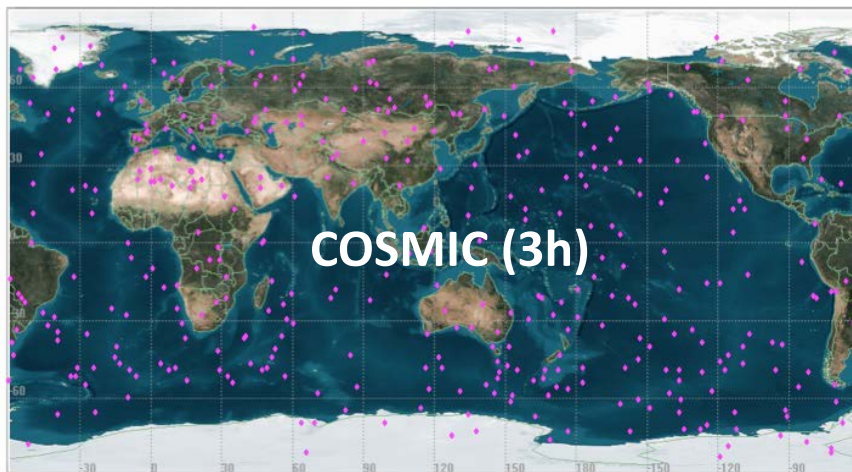
Total atmospheric occultations: 6,624,788



COSMIC-II 2017

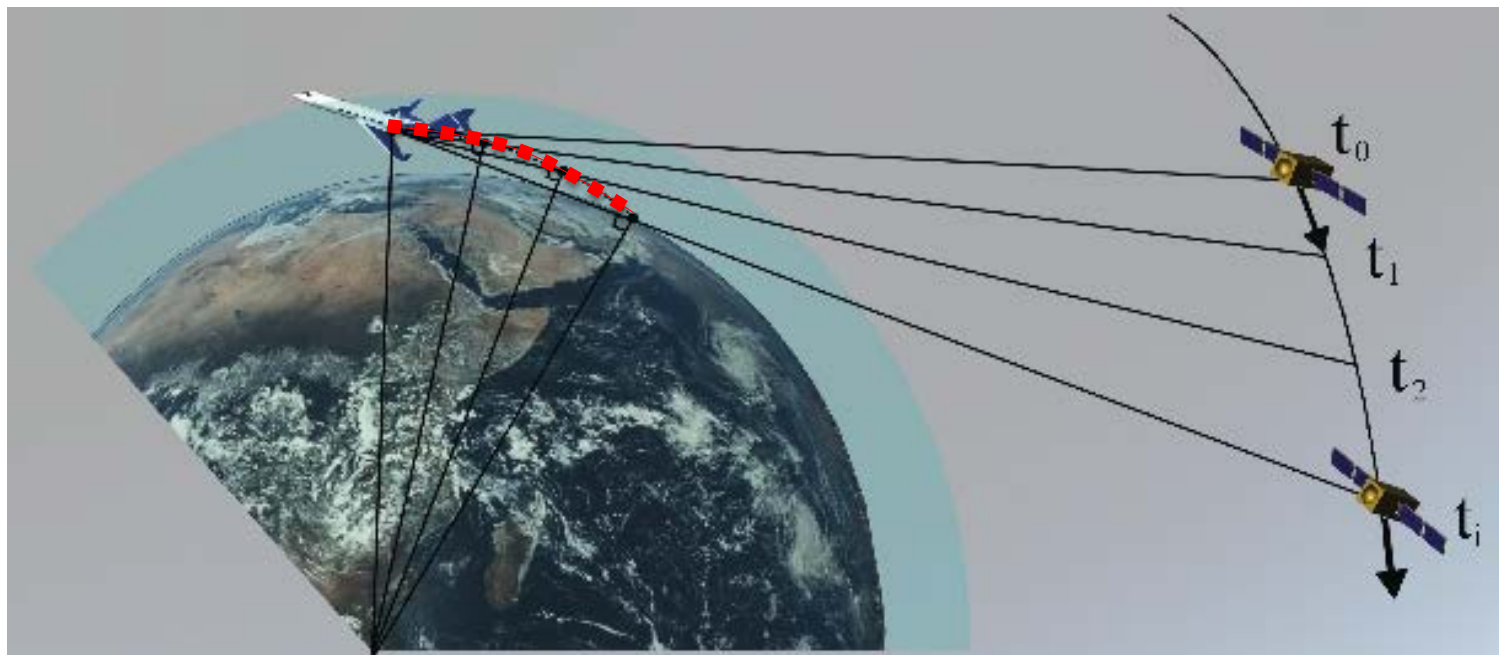
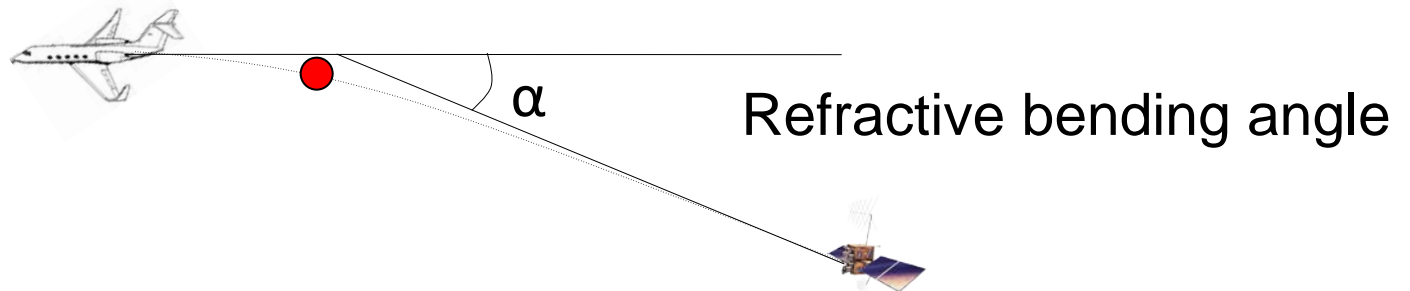


UCAR COSMIC



Air-borne GPS RO

Side-looking GPS receiver tracks setting and rising satellites



Motivation

- GPS RO measurements are nearly weather free. Studies have shown that the assimilation of spaceborne GPS RO data can improve large-scale features.
- However, the coverage of the spaceborne GPS RO data are sparse for mesoscale applications. Thus a GPS RO receiver was placed on the NSF/NCAR GV aircraft during the PREDICT* field campaign in 2010 to collect denser GPS RO data for tropical cyclone studies.

* *PREDICT: PRE-Depression Investigation of Cloud-systems in the Tropics*

Objective

- Investigate the impact of assimilating airborne GPS RO data on Hurricane Karl (2010) forecast using different observational operators.

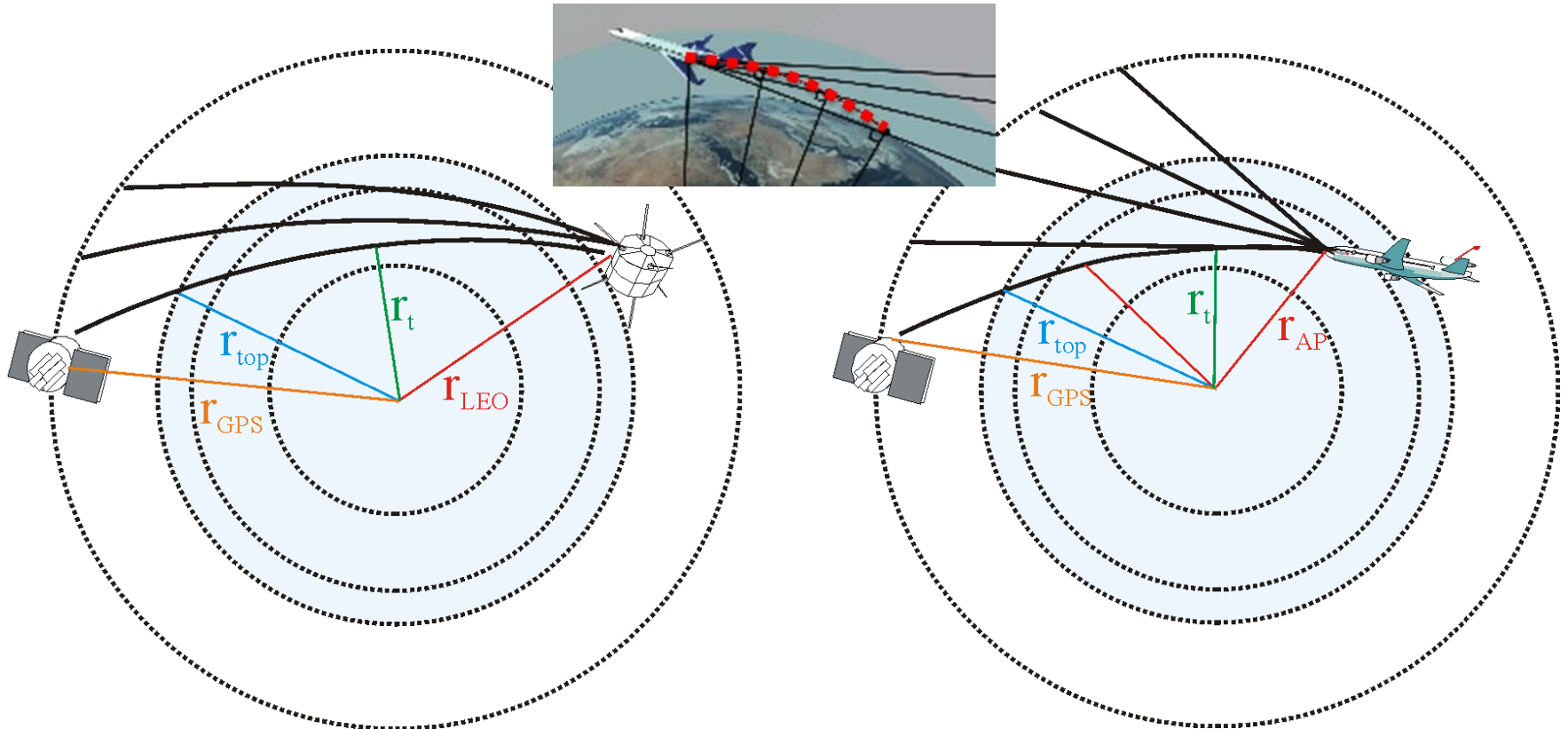
GISMOS Installed on NSF/NCAR GV



“*GISMOS*” (GNSS [Global Navigation Satellite System] Instrument System for Multistatic and Occultation Sensing)

Spaceborne (L) vs. Air-borne (R) GPS ROs

ARO's tangent points horizontally drift 2-3 times of SRO's

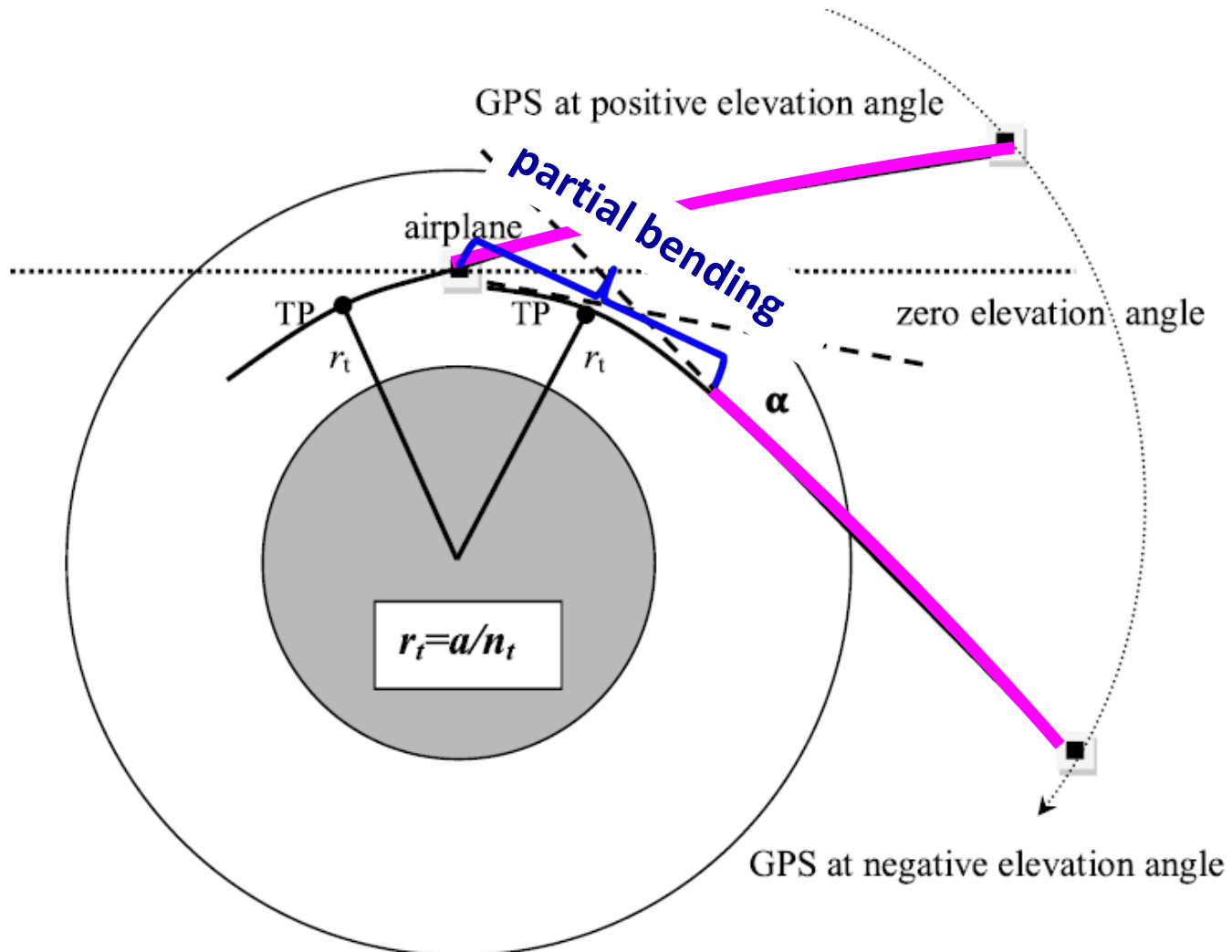


$$\alpha = 2 \int_{r_t}^{r_{top}} \frac{1}{\sqrt{n^2 r^2 - a^2}} \frac{d(\ln n)}{dr} dr$$

$$\alpha = \int_{r_t}^{r_{AP}} \frac{1}{\sqrt{n^2 r^2 - a^2}} \frac{d(\ln n)}{dr} dr + \int_{r_t}^{r_{top}} \frac{1}{\sqrt{n^2 r^2 - a^2}} \frac{d(\ln n)}{dr} dr$$

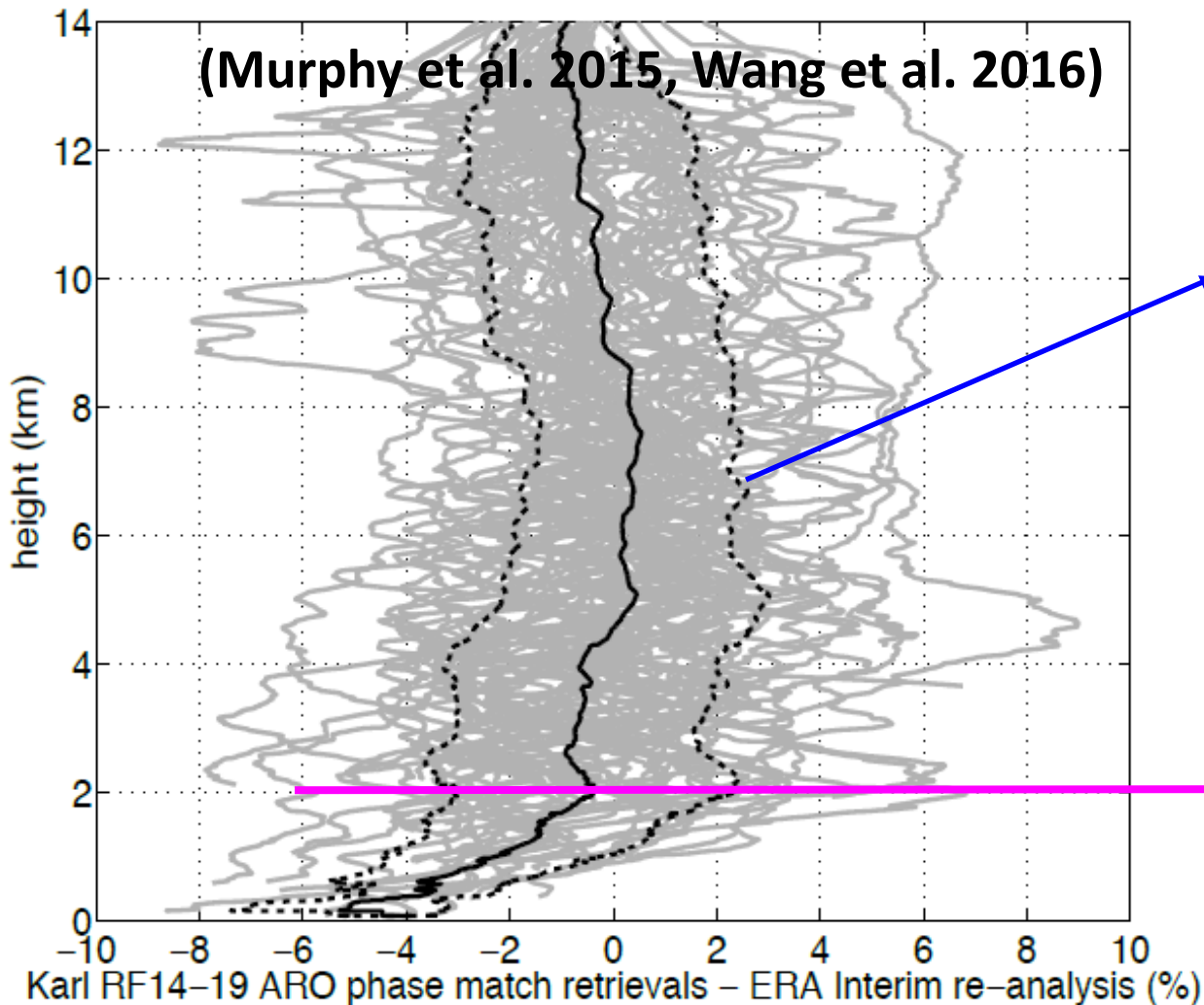
Airborne GPS ROs

Removing the effect of the atmosphere above the airplane level



ARO FSI Retrieval vs. ERA-Interim

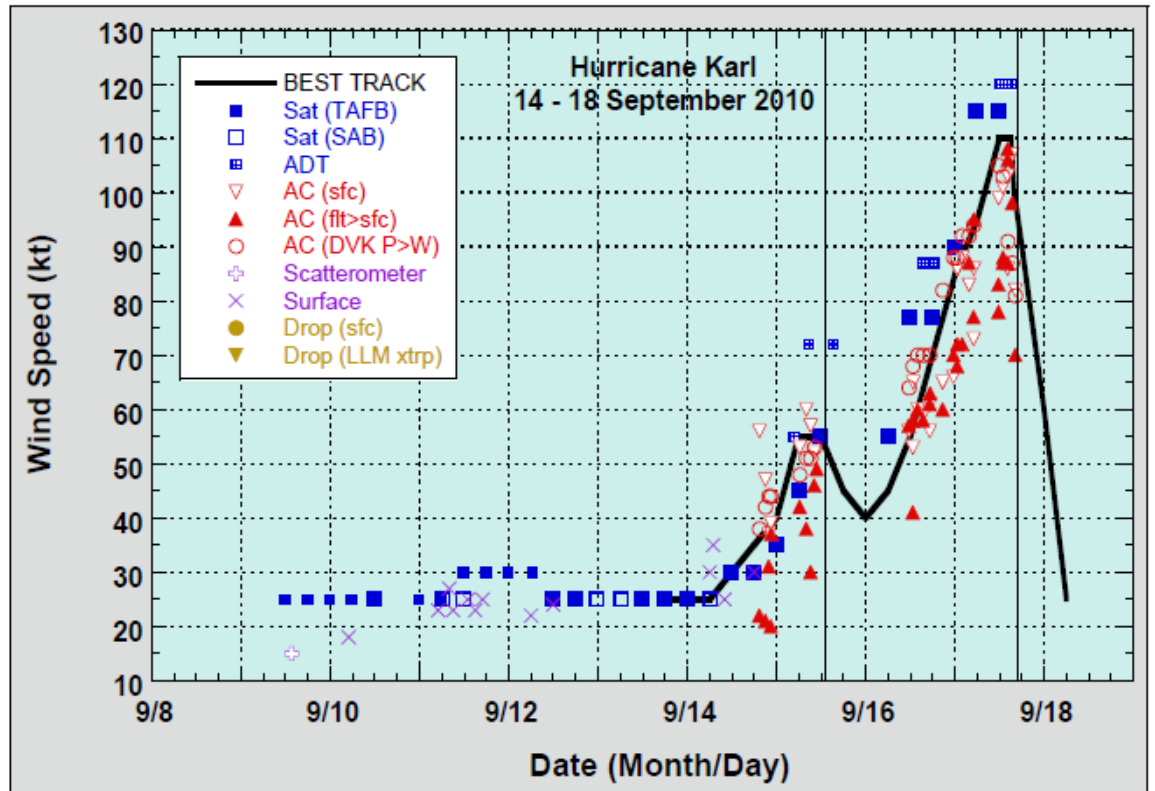
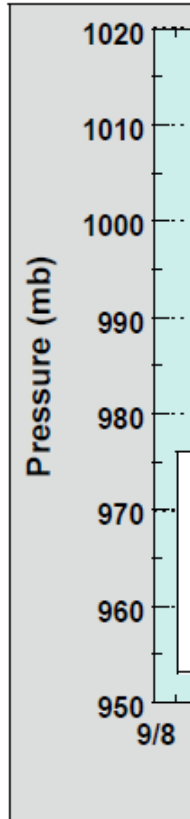
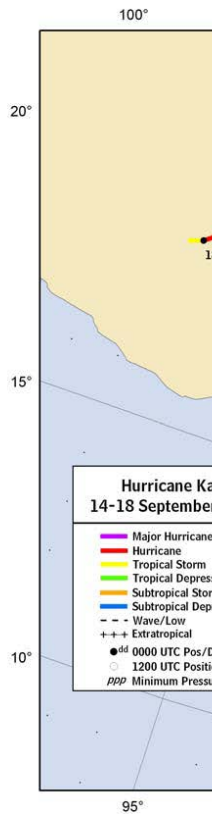
Retrievals from open-loop tracking and phase matching (PM)



~ 2% standard deviation in the difference between the retrieved ARO refractivity and the ERA-Interim reanalysis.

Apparent bias at low levels below 2km, possibly from multipath issues.
(Data are discarded in data assimilation)

Case study: Hurricane Karl 2010



NHC/NOAA

Figure 3.

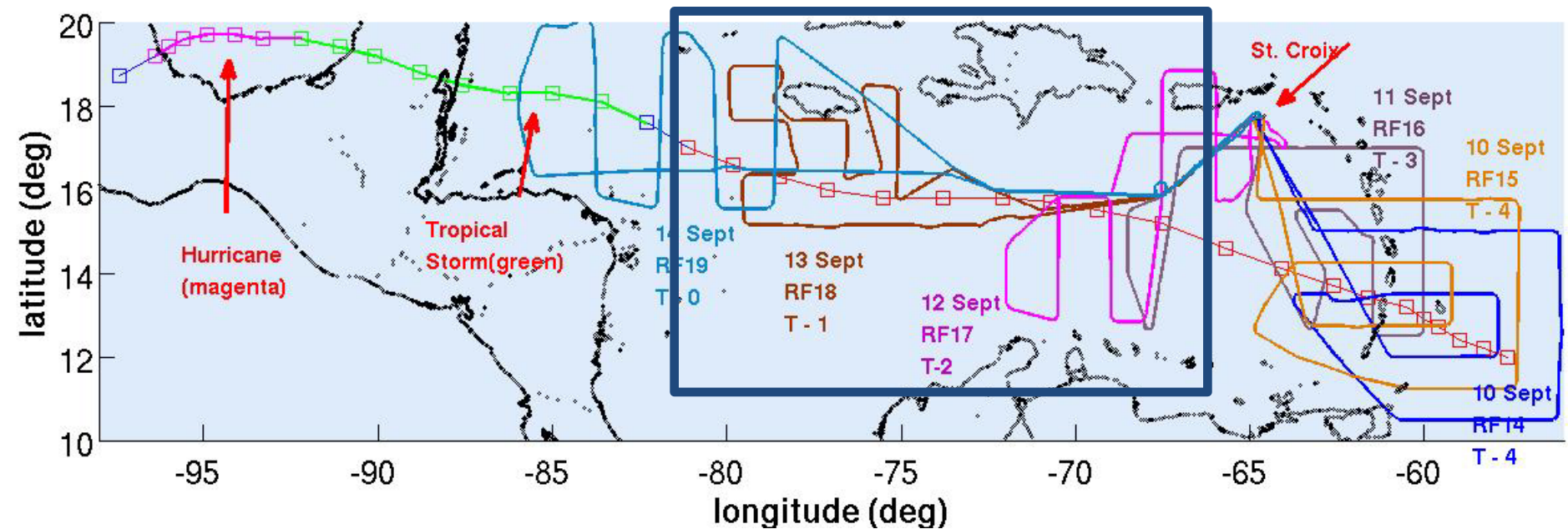
Selected pressure observations from 2010. Advanced Dvorak observation

Figure 2.

Selected wind observations and best track maximum sustained surface wind speed curve for Hurricane Karl, 14-18 September 2010. Aircraft observations have been adjusted for elevation using 90%, 80%, and 80% adjustment factors for observations from 700 mb, 850 mb, and 1500 ft, respectively. Advanced Dvorak Technique estimates represent linear averages over a two-hour period centered on the nominal observation time. Dashed vertical lines correspond to 0000 UTC. Solid vertical lines correspond to landfall times.

Case study: Hurricane Karl 2010

6 flights into pre-Hurricane Karl



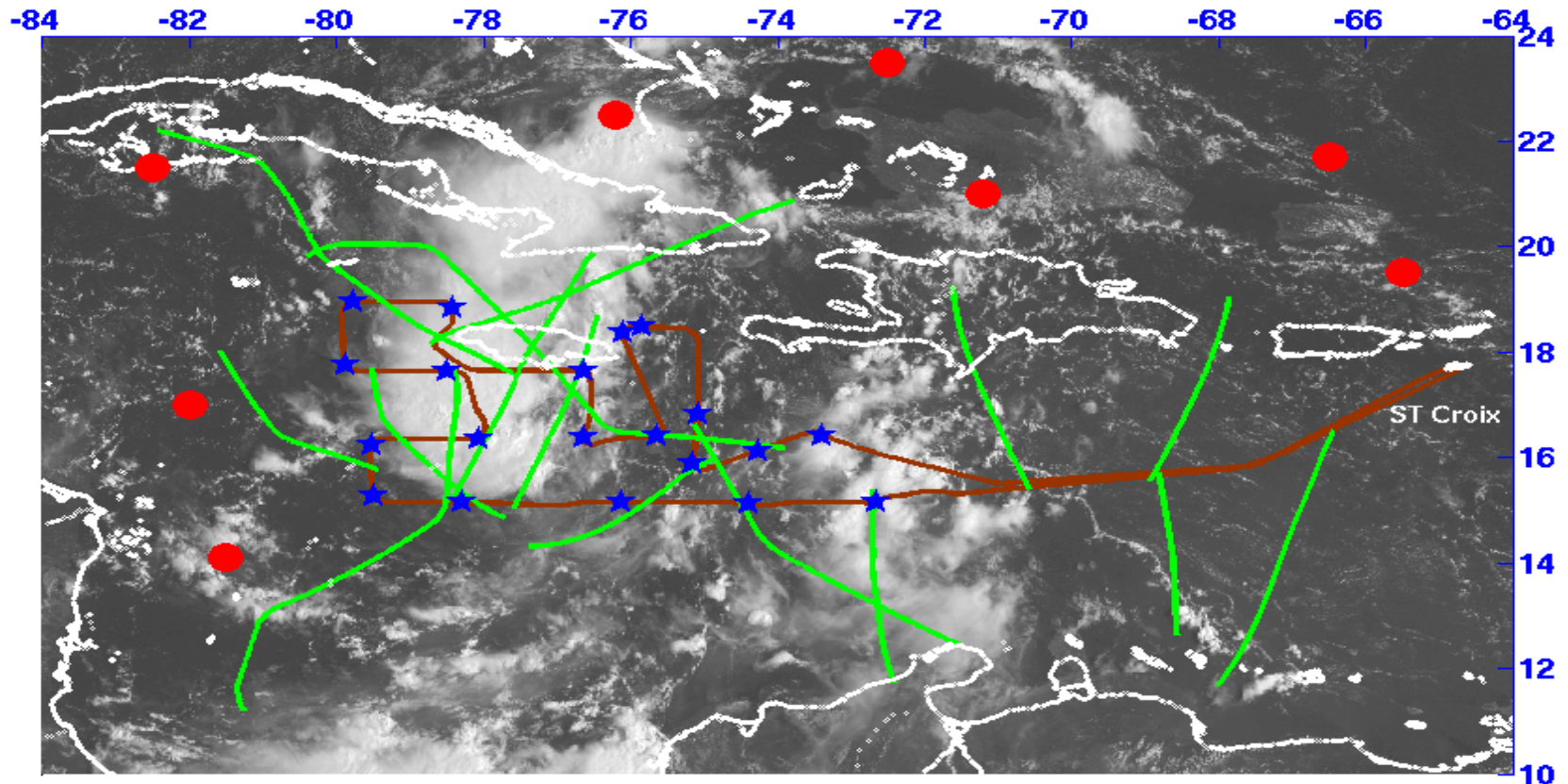
Flight RF18 (Sep 13): ~1 day before Karl genesis

PREDICT – Airborne GPS RO vs COSMIC

● COSMIC

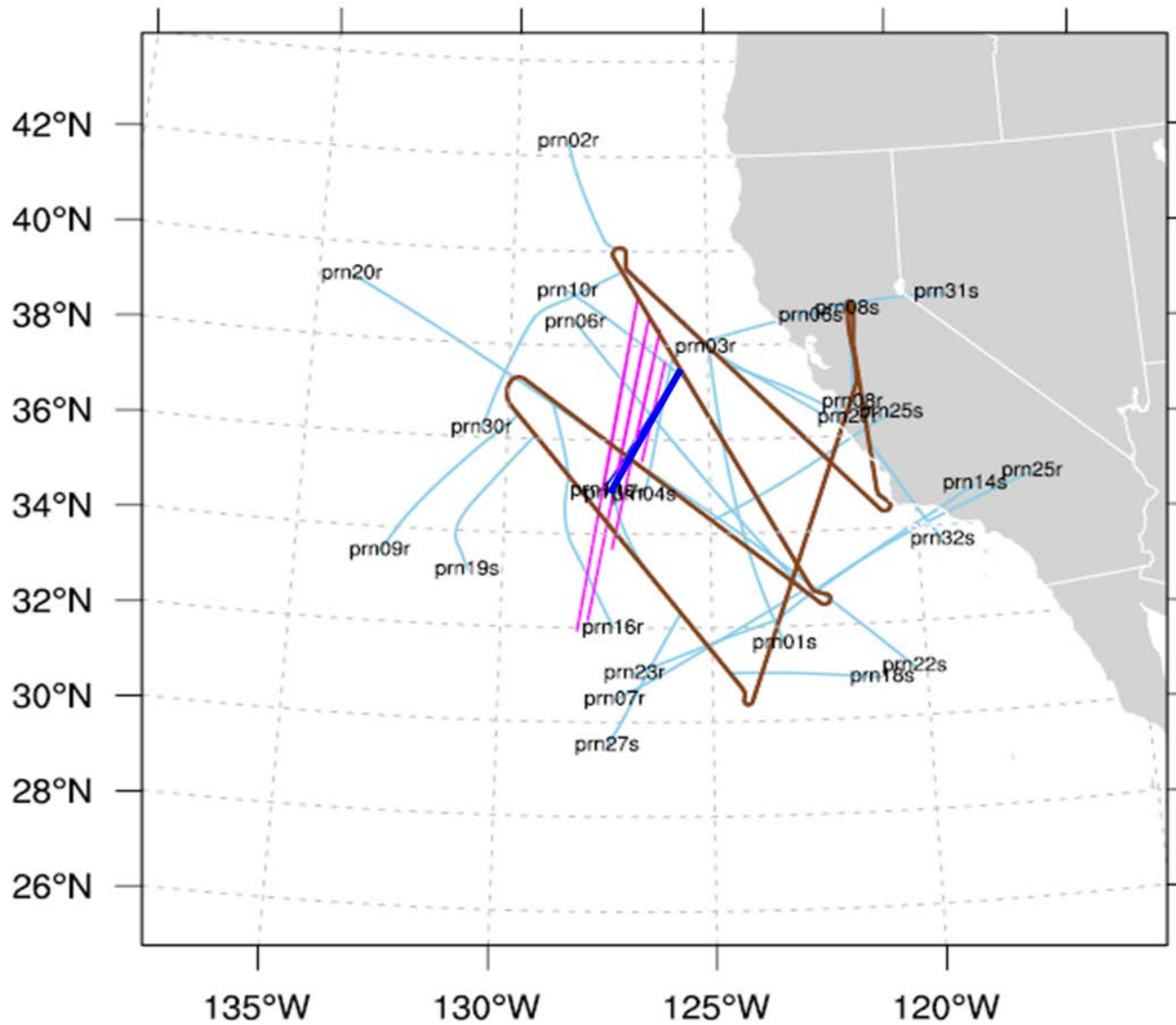
— ARO

★ Dropsonde

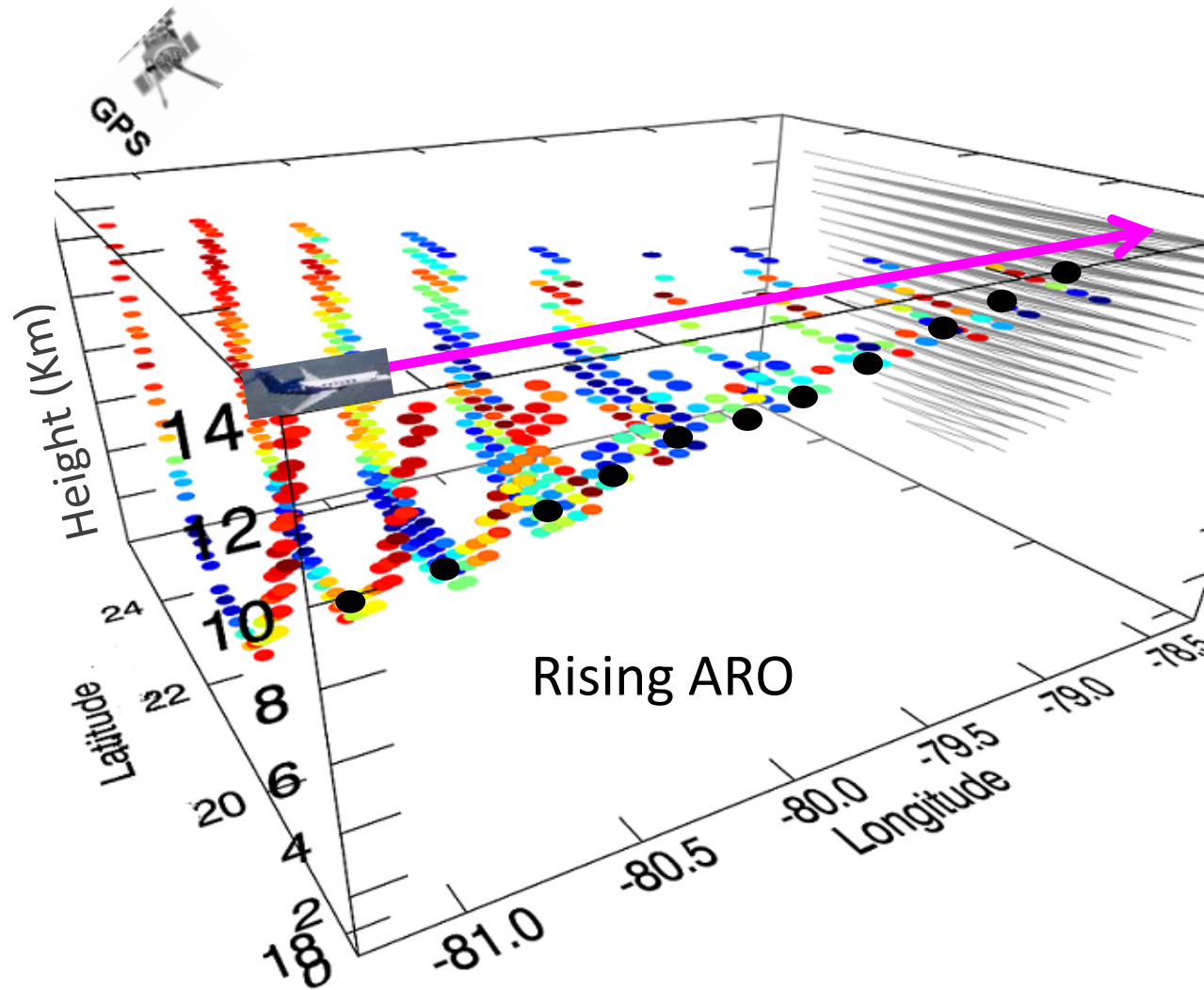


Flight RF18 (Sep 13): ~1 day before Karl genesis

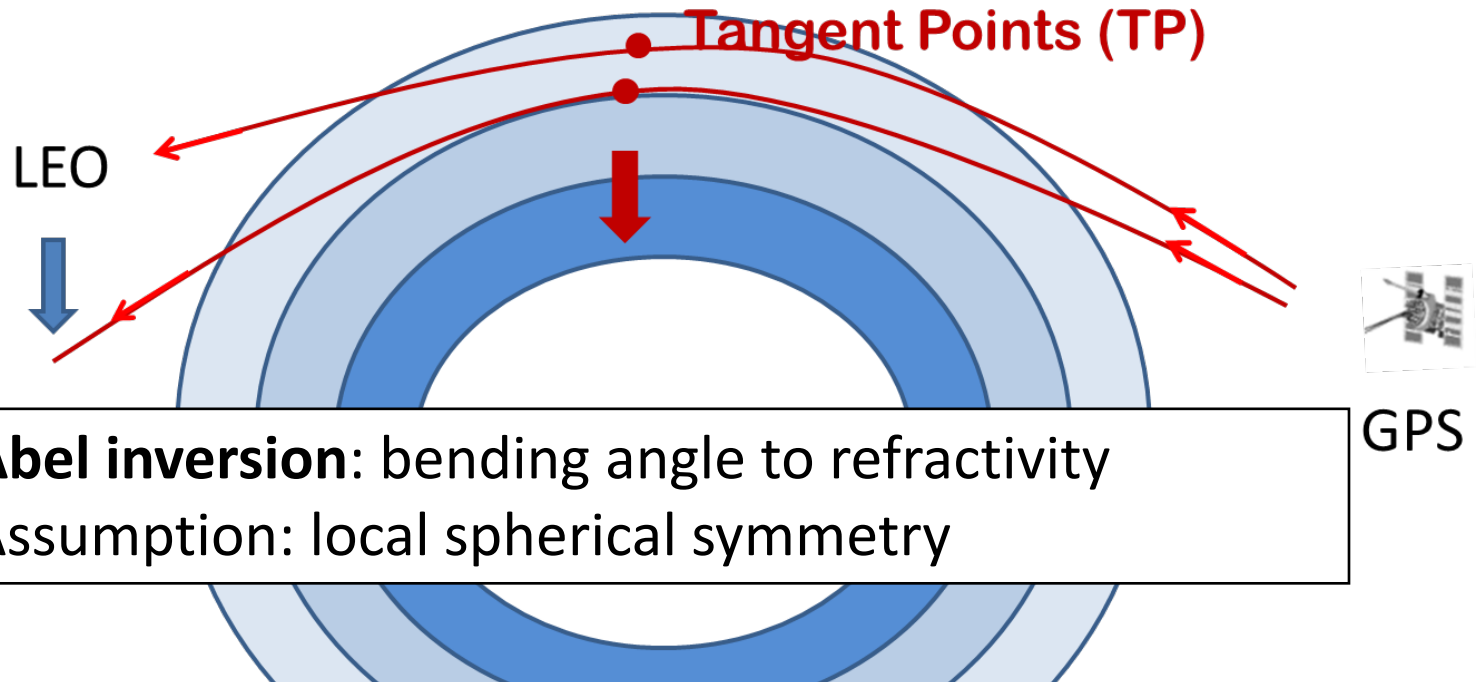
Airborne GPS RO Rays



Data: Refractivity vs. Excess Phase



Data: Refractivity vs. Excess Phase



Abel inversion: bending angle to refractivity
Assumption: local spherical symmetry

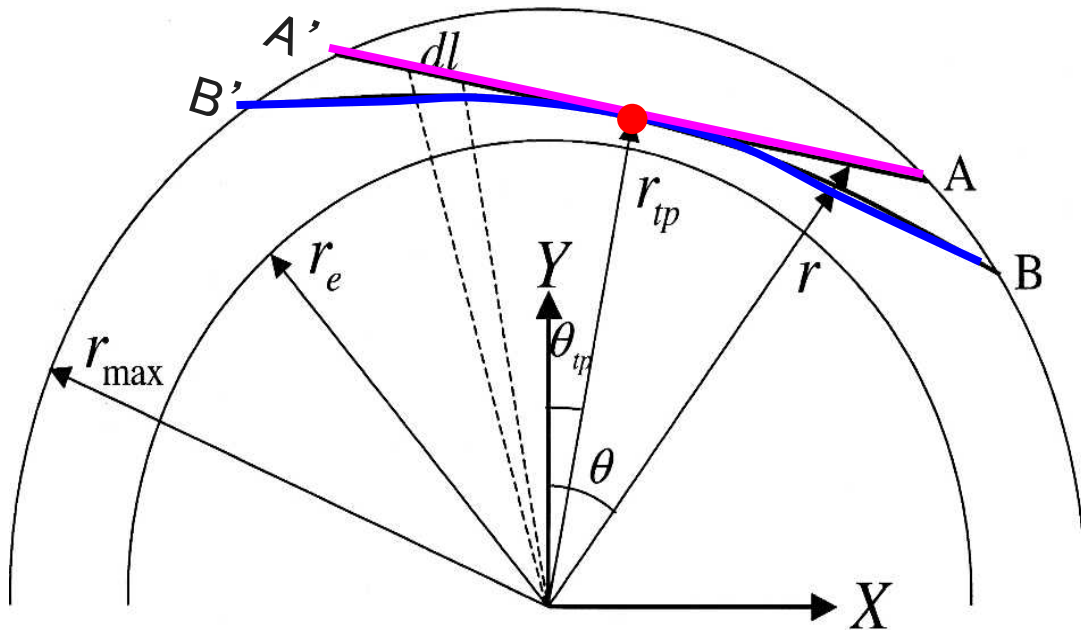
How are we going to use the data after knowing their basic characteristics?

Observable = phase data \Rightarrow Doppler shift
 \Rightarrow bending angle \Rightarrow refractivity

Data: Refractivity vs. Excess Phase

Non-Local Operator
(Excess phase)

$$EPH \approx \int_{A'}^A N ds$$

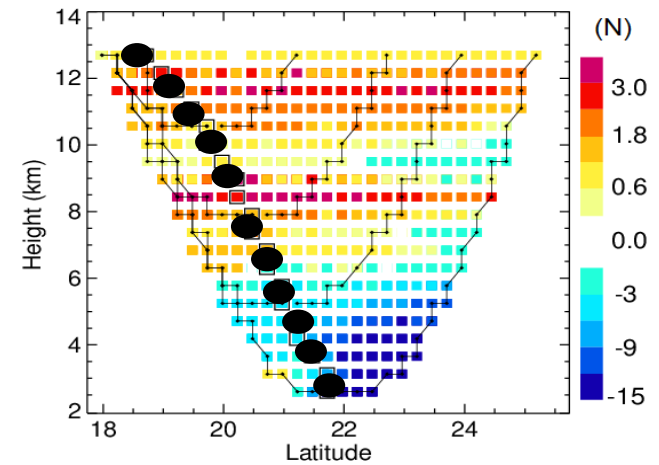
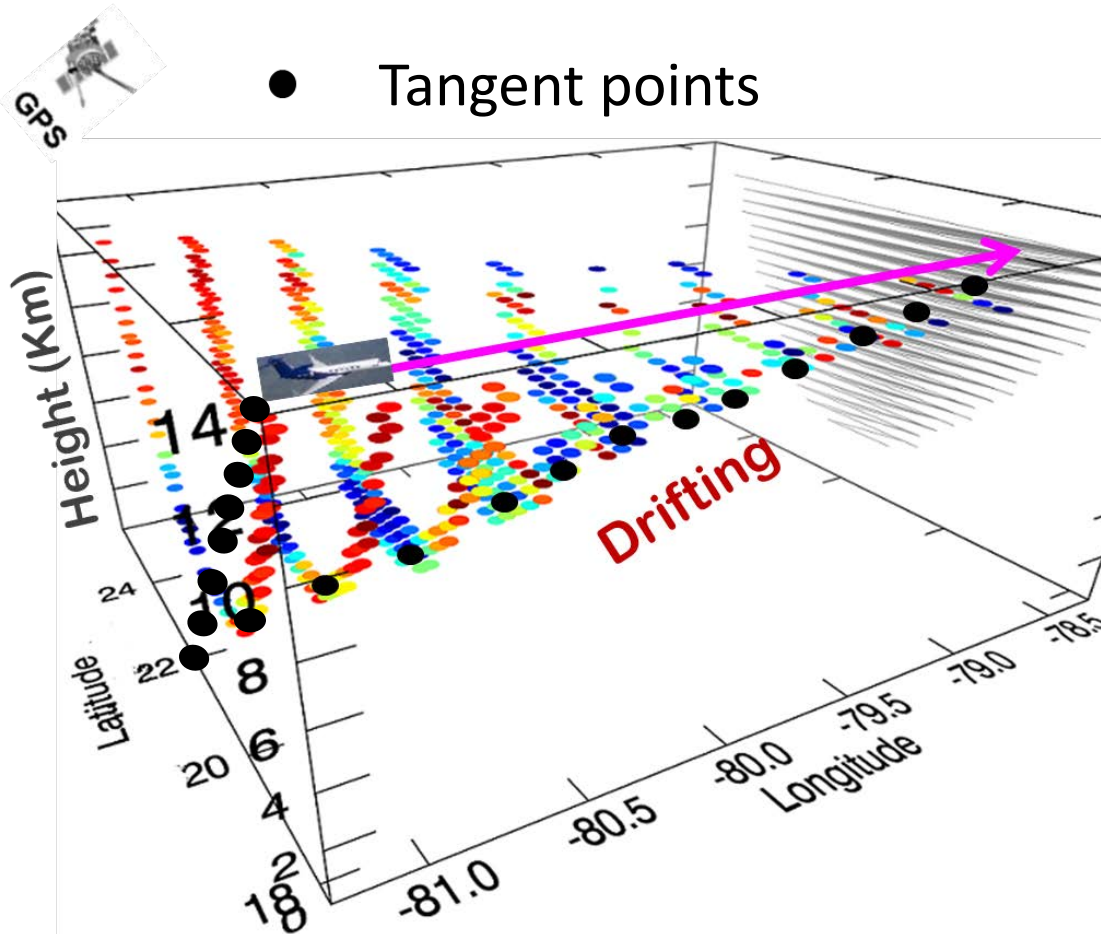


Local operator
(Refractivity)

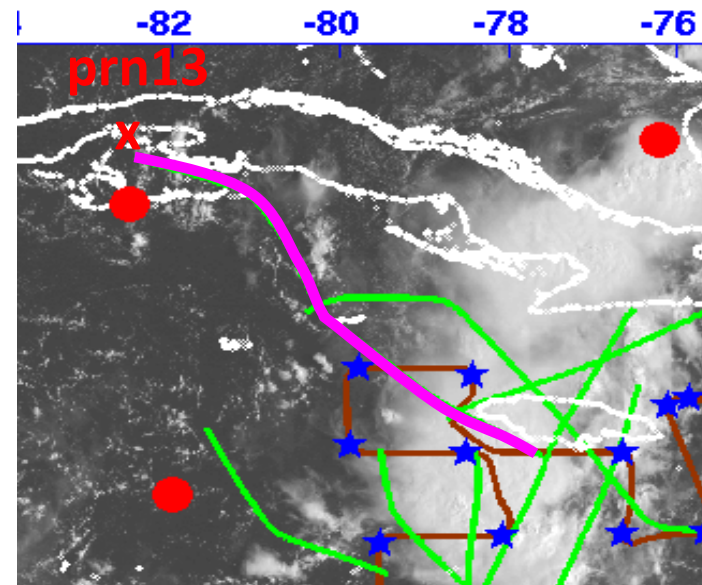
$$N \approx 77.6 \frac{P}{T} + 3.73 \times 10^5 \frac{P_w}{T^2}$$

Sokolovskiy et al. 2005

Drifting vs. Non-Drifting Tangent Points



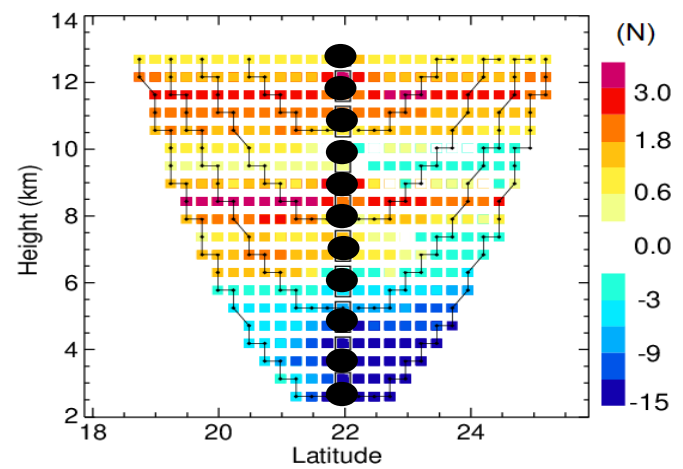
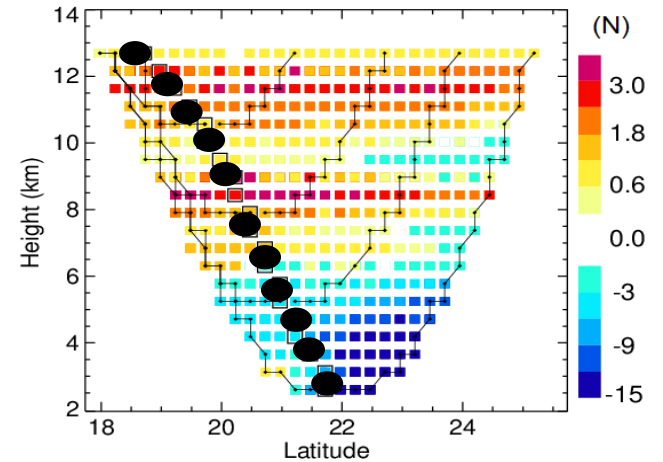
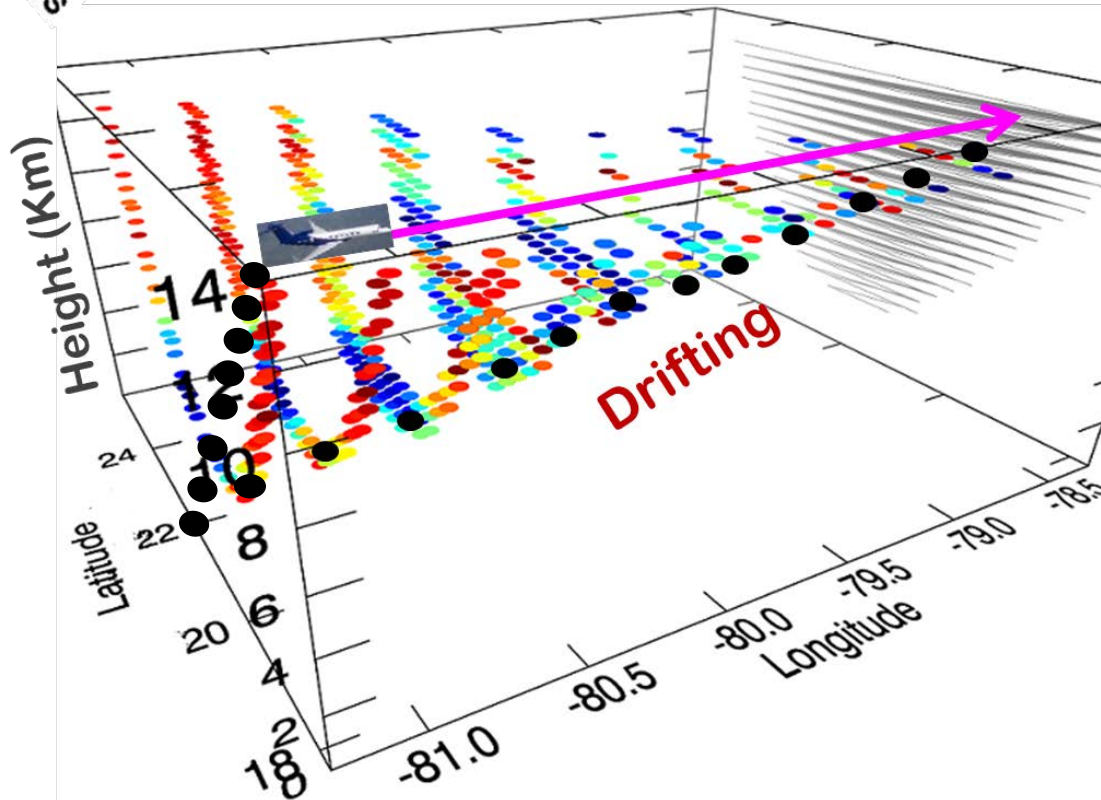
Drifting (projected to a 2D plane)



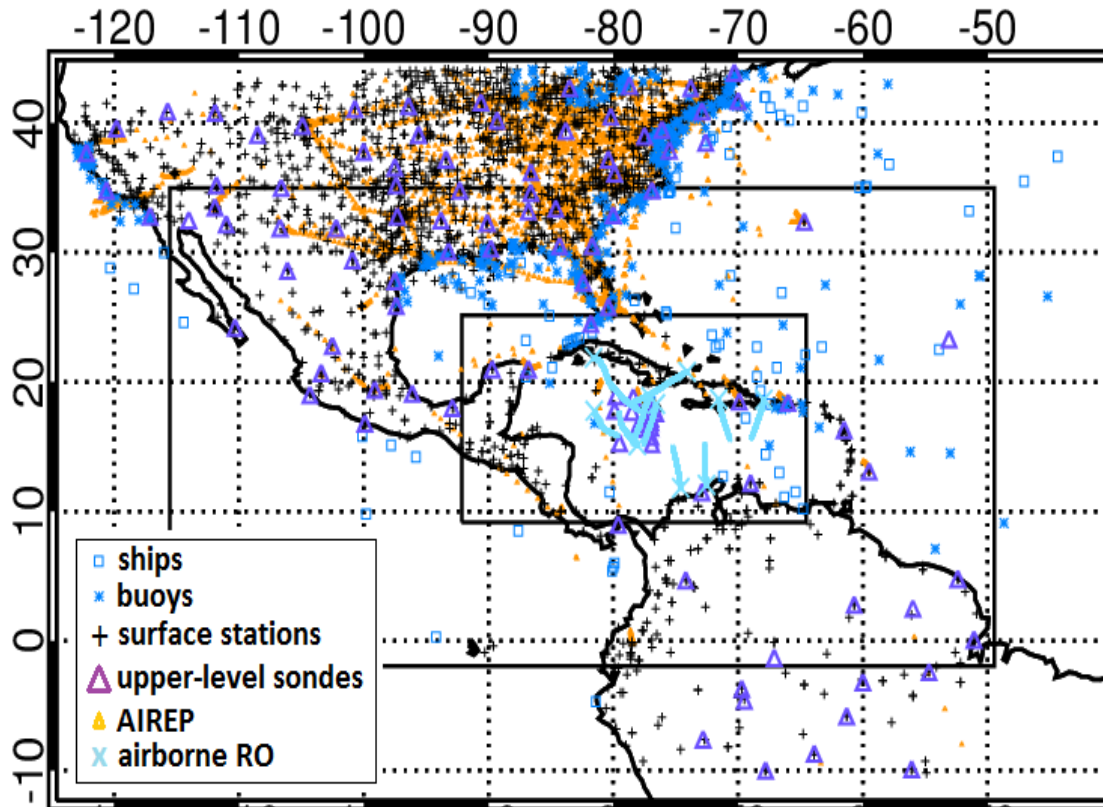
Drifting vs. Non-Drifting Tangent Points



- Tangent points



Numerical Experiments



WRFV3.2, WRF 3DVAR with modified GPSRO operator for airborne receiver, based on the one for spaceborne (Chen et al. 2009).

**Resolution: 27, 9, 3km
Vortex following**

| | |
|---------------------|-----------------|
| Microphysics | Morrison |
|---------------------|-----------------|

| | |
|------------|------------|
| PBL | YSU |
|------------|------------|

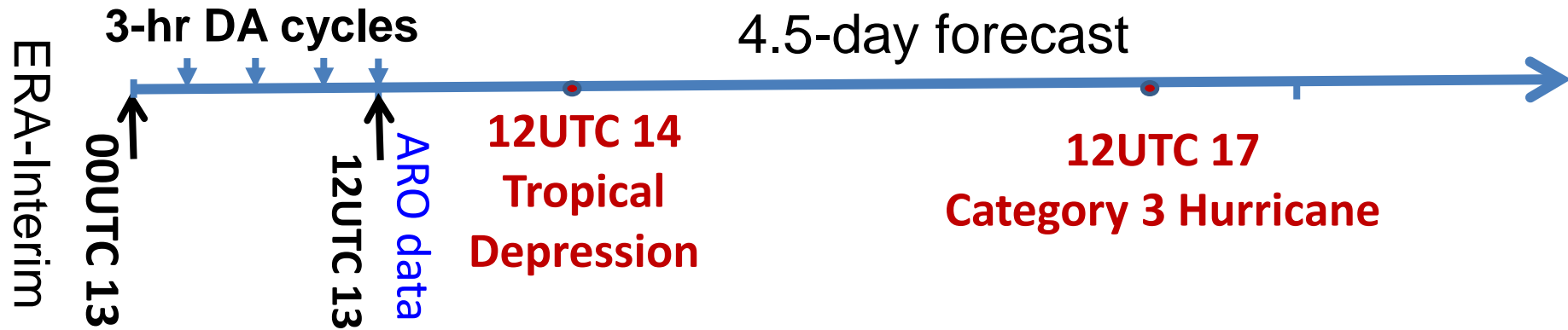
| | |
|---------------------------|---------------------|
| Cumulus (d01, d02) | Kain-Fritsch |
|---------------------------|---------------------|

| | |
|-----------------|-------------|
| Longwave | RRTM |
|-----------------|-------------|

| | |
|------------------|----------------|
| Shortwave | Goddard |
|------------------|----------------|

BE: 60 pairs of 12 and 24-hr WRF forecast differences (NMC-method).

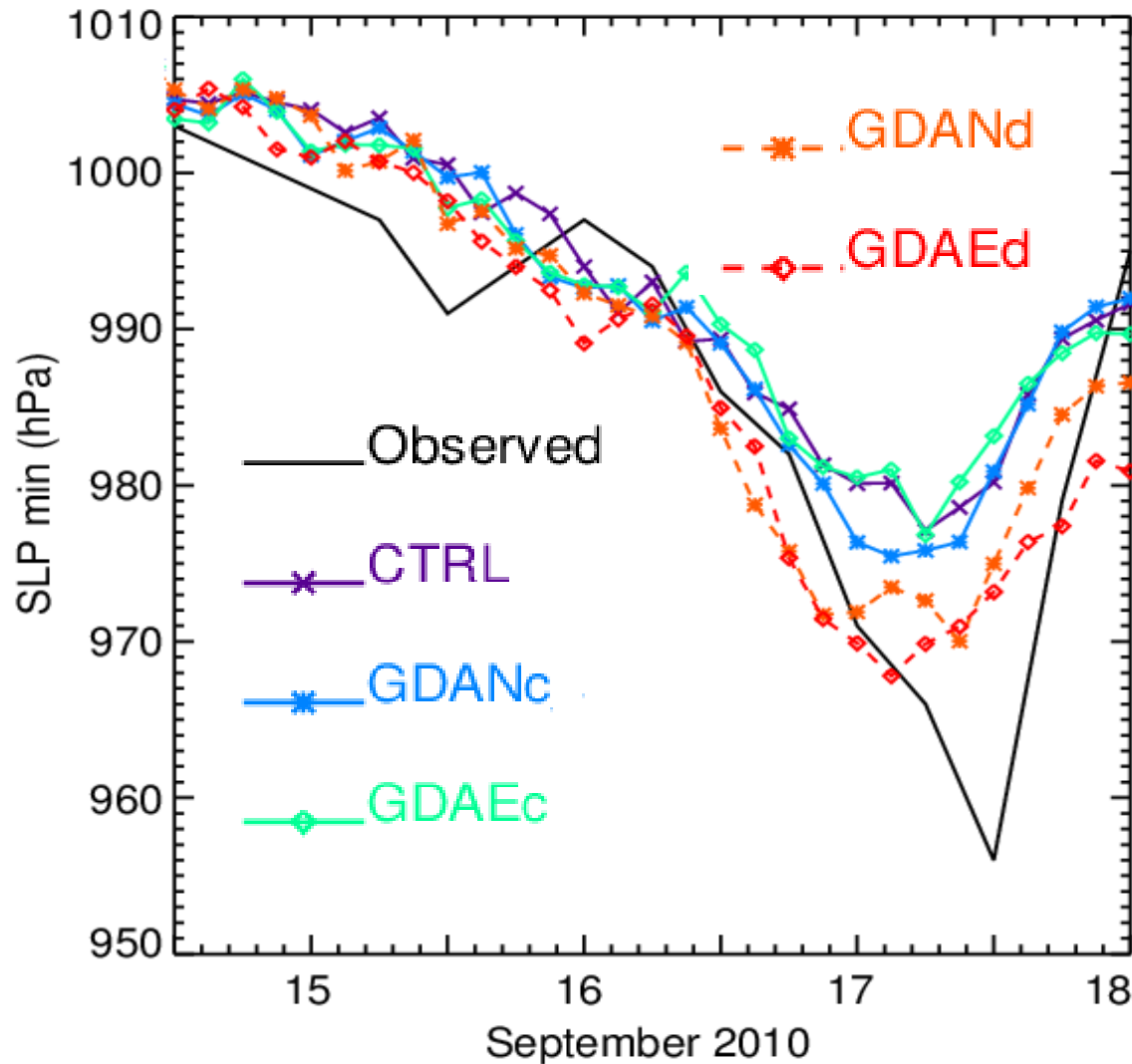
Numerical Experiments



| <i>Exp.</i> | <i>Observations assimilated</i> |
|--------------|---|
| CTRL | GTS + dropsondes |
| GDANc | CNTL data + ARO local refractivity with no drifting of tangent points (i.e. column data), 2% error |
| GDANd | Same as GDANc, except with drifting tangent points |
| GDAEc | CNTL data + ARO excess phase with column data, 1% error |
| GDAEd | Same as GDAEc, except with drifting tangent points |

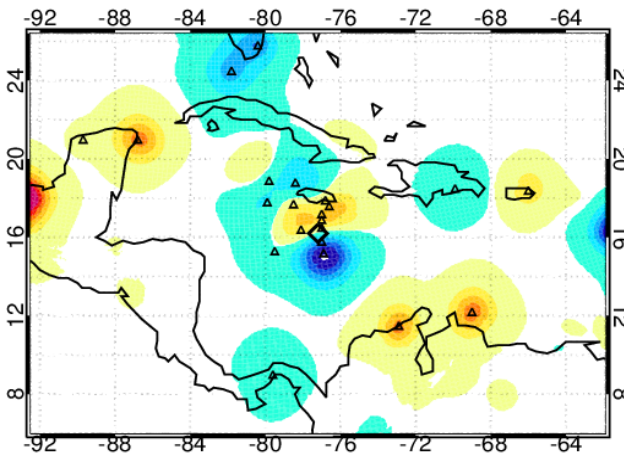
Intensity Forecast (Min SLP)

1200 UTC 14 Sept. – 0000 UTC 18 Sept. 2010

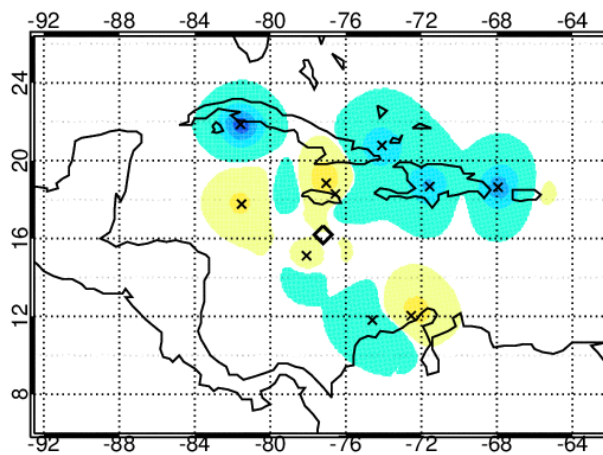


TPW Analysis Differences (12Z Sep 13)

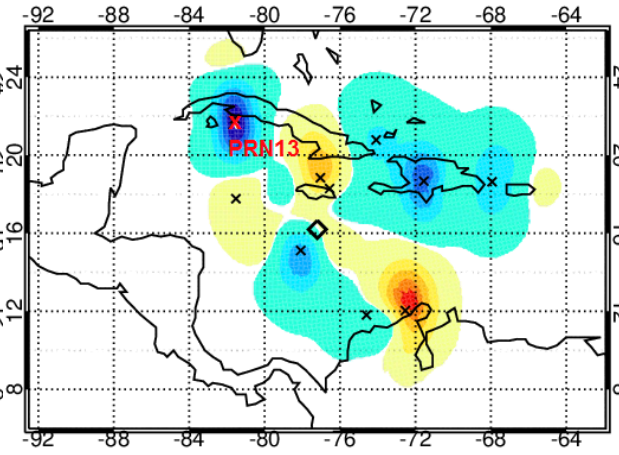
CTRL
Analysis Increment



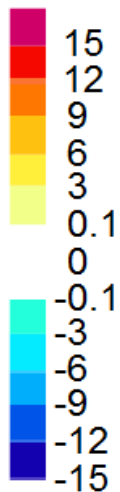
GDANc – CTRL



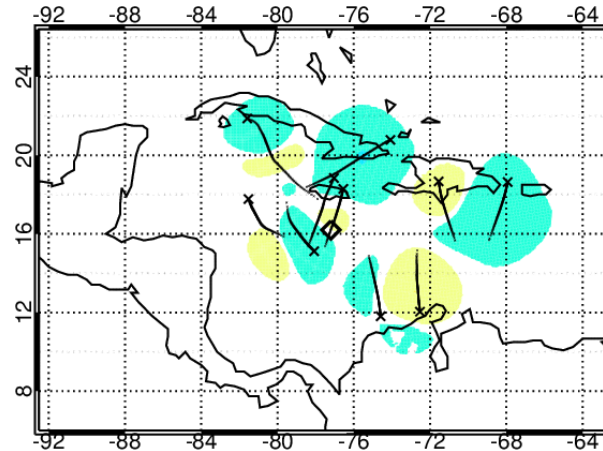
GDAEc – CTRL



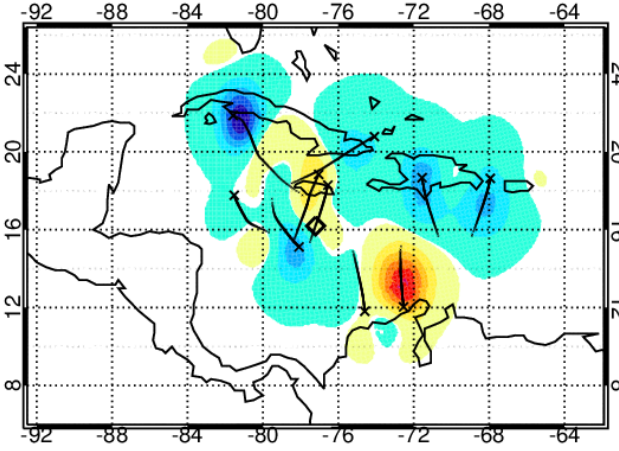
TPW (%)



GDANd – CTRL

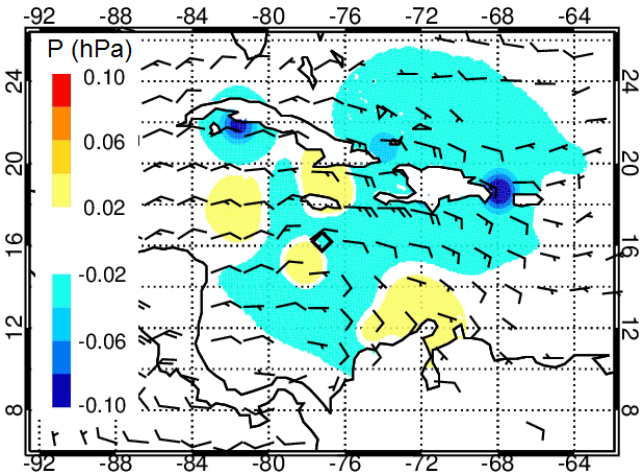


GDAEd – CTRL

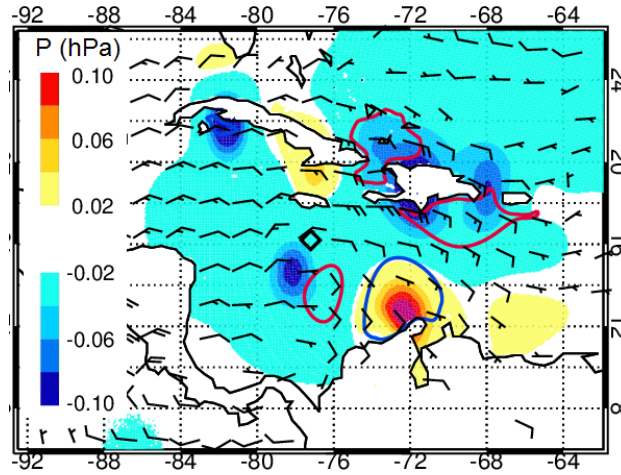


Analysis Differences @ 3 km

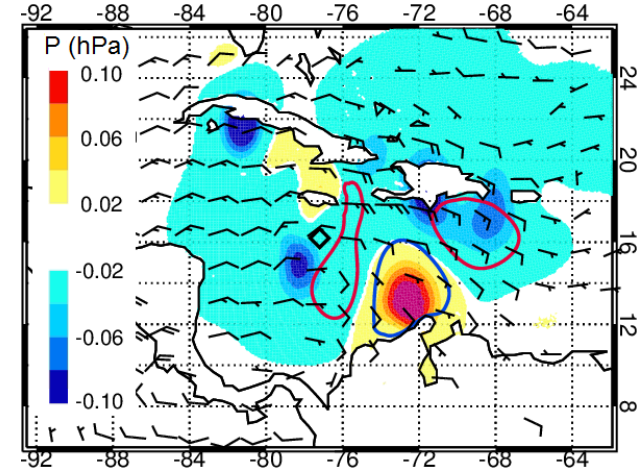
GDANc – CTRL, P, vor



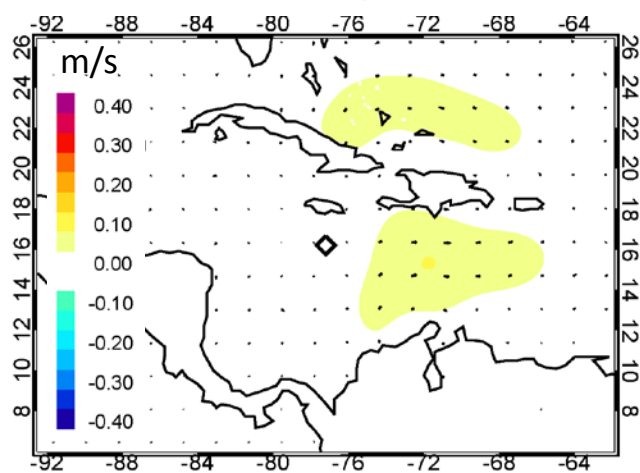
GDAEc – CTRL, P, vor



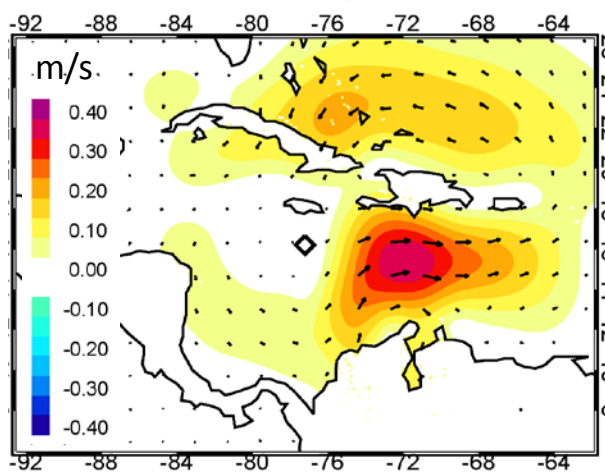
GDAEd – CTRL) P, vor



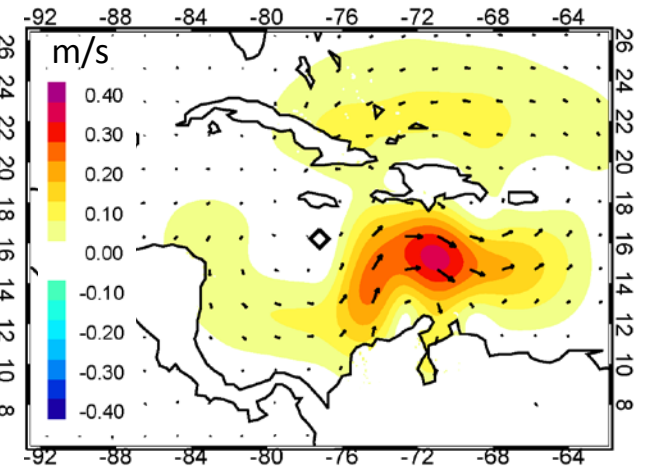
GDANc – CTRL, wind



GDAEc – CTRL, wind

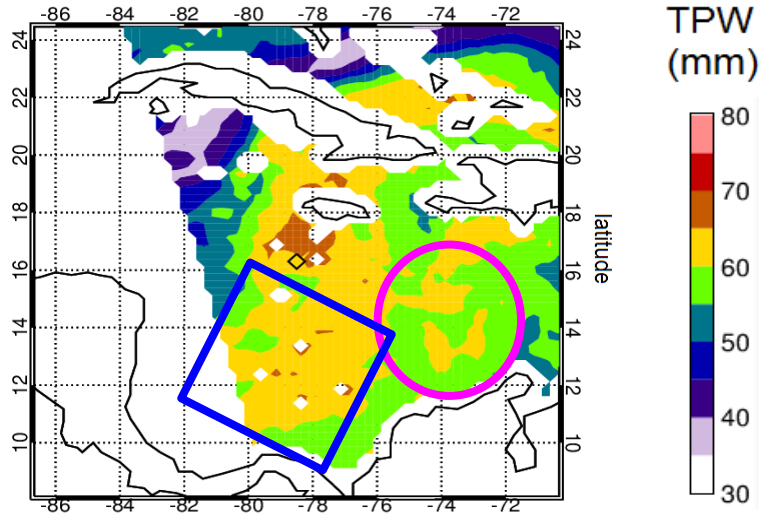


GDAEd – CTRL, wind



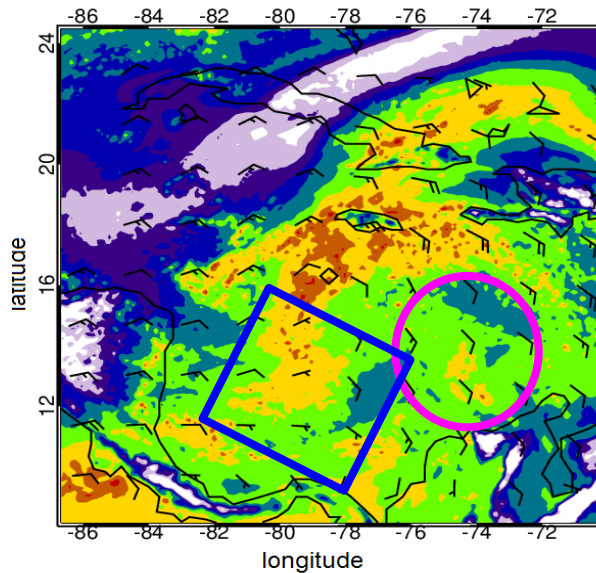
6-h TPW Forecasts (18Z 13 Sep.)

Composite Satellite Data

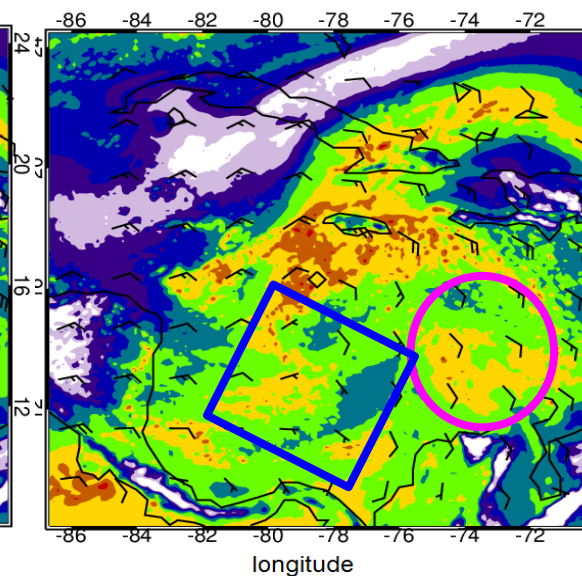


Torn and Cook (2013) found that the 48-h forecasts of Karl were particularly sensitive to initial mid-level moisture perturbations southeast of the storm north of Colombia and Venezuela.

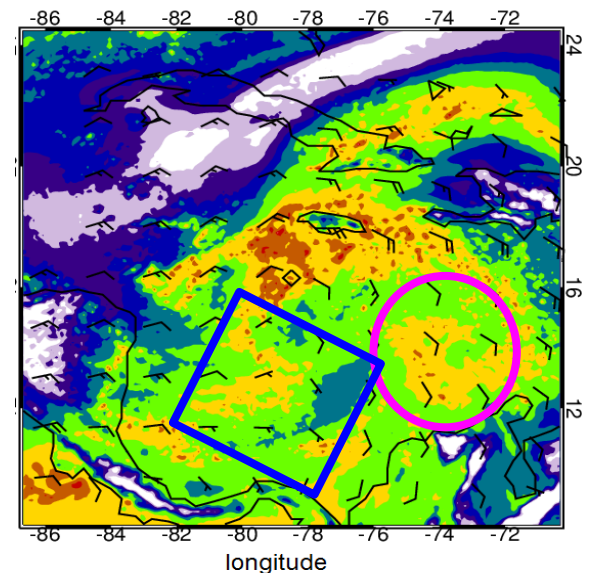
CTRL



GDAEc

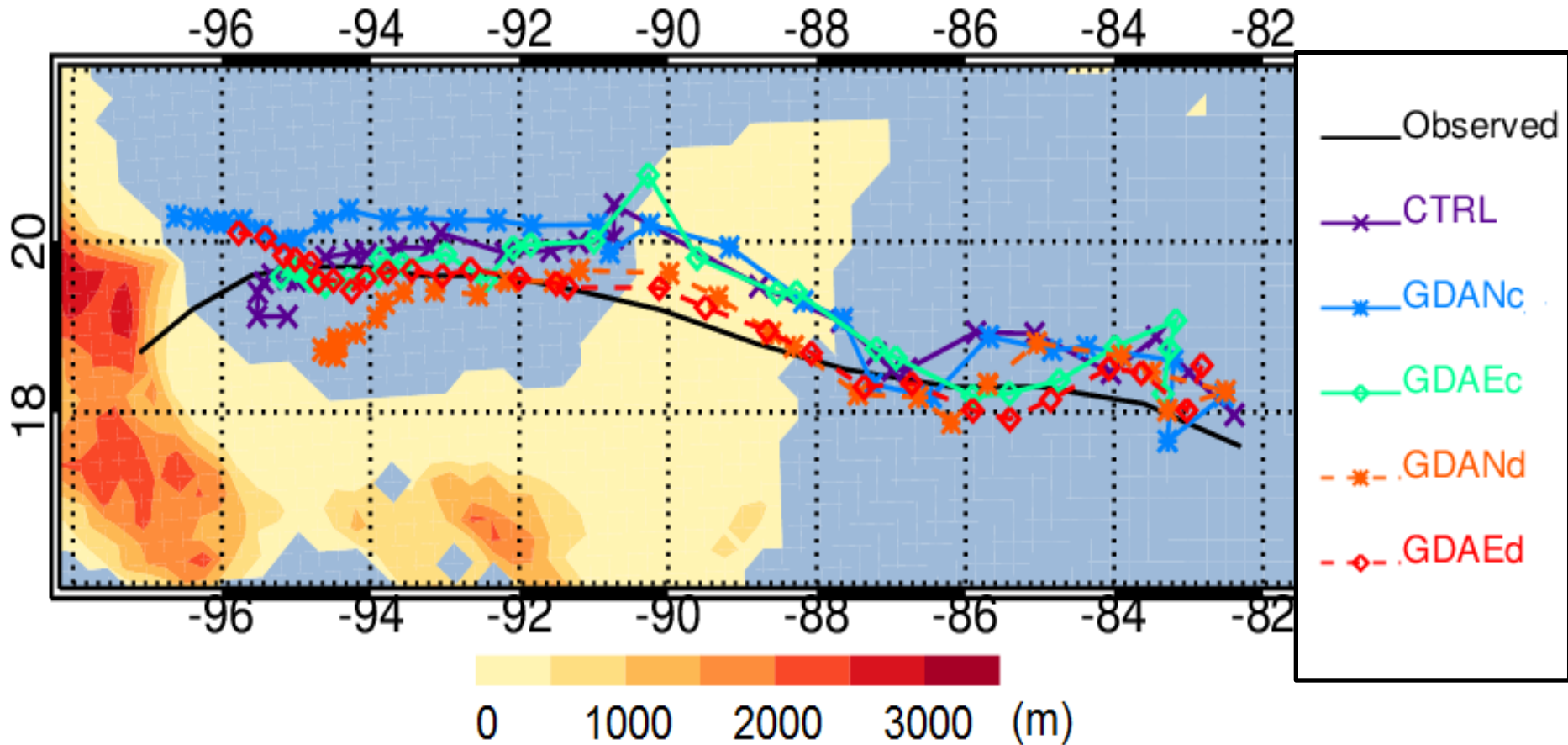


GDAEd



Track Forecasts

1200 UTC 14 Sept. – 0000 UTC 18 Sept. 2010

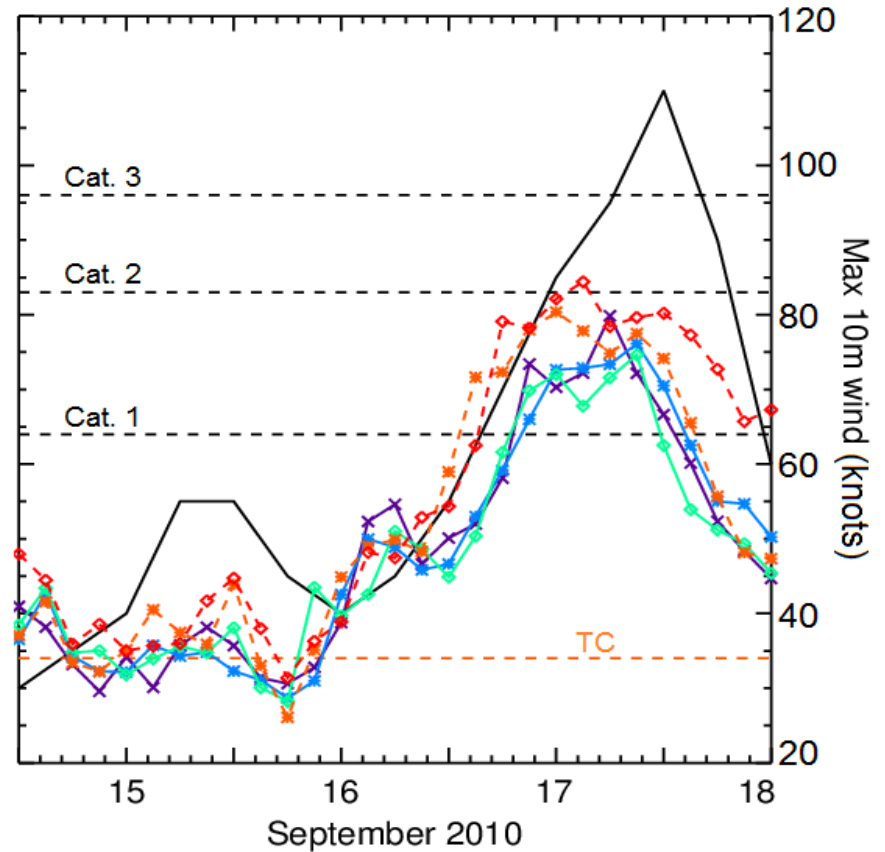
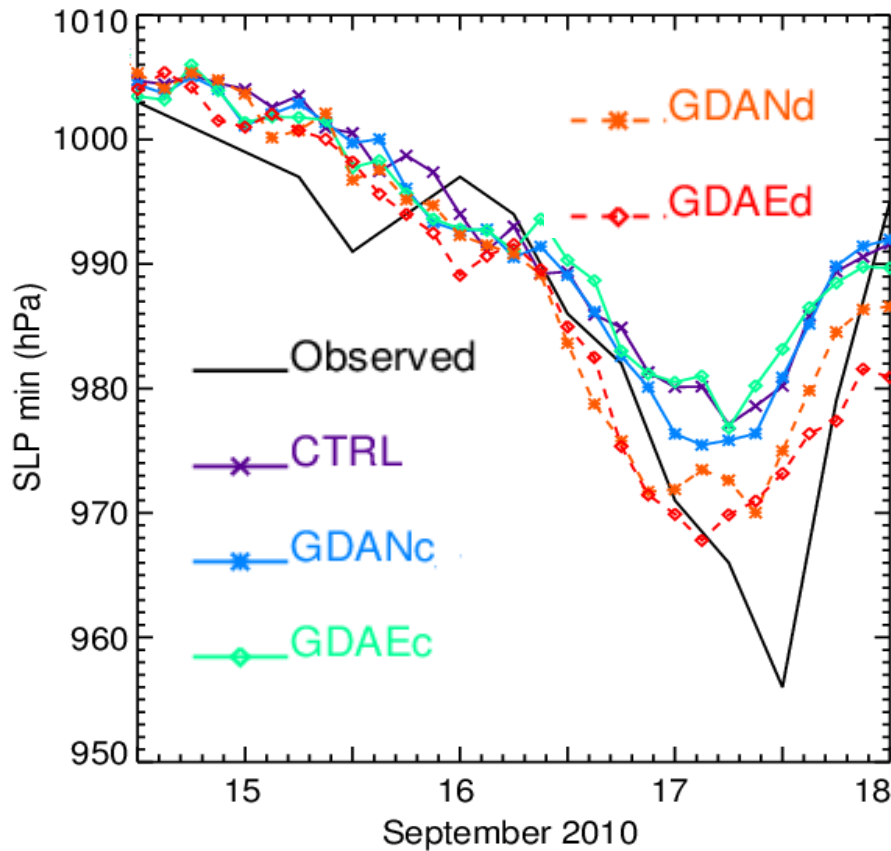


Intensity Forecasts

1200 UTC 14 Sept. – 0000 UTC 18 Sept. 2010

Min SLP

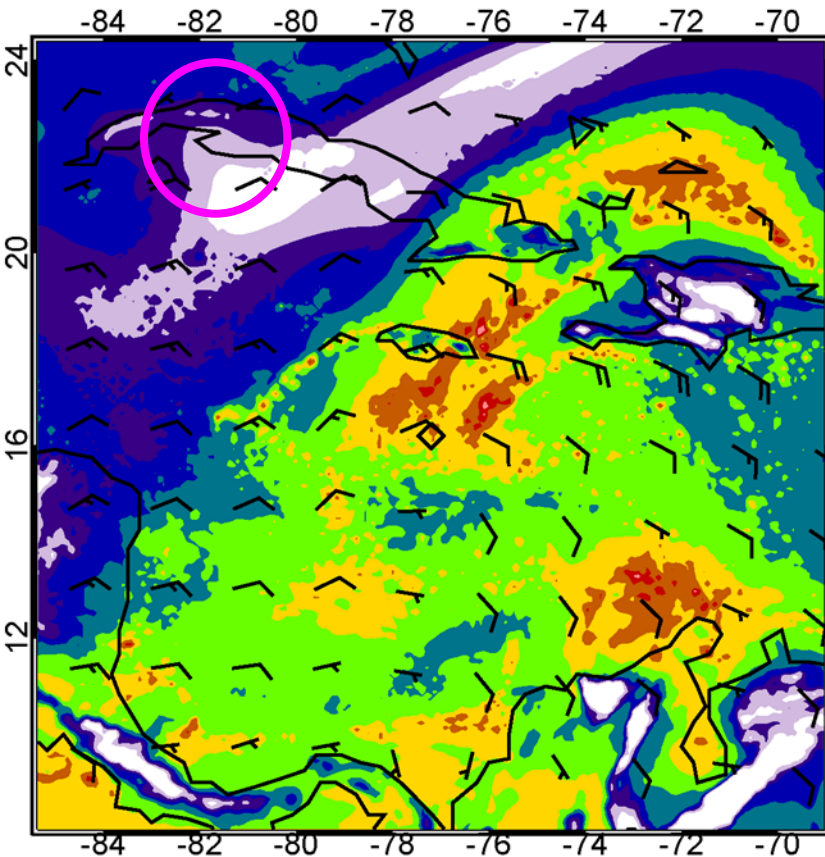
10-m wind speed



TPW Analysis (12Z 13 Sep.)

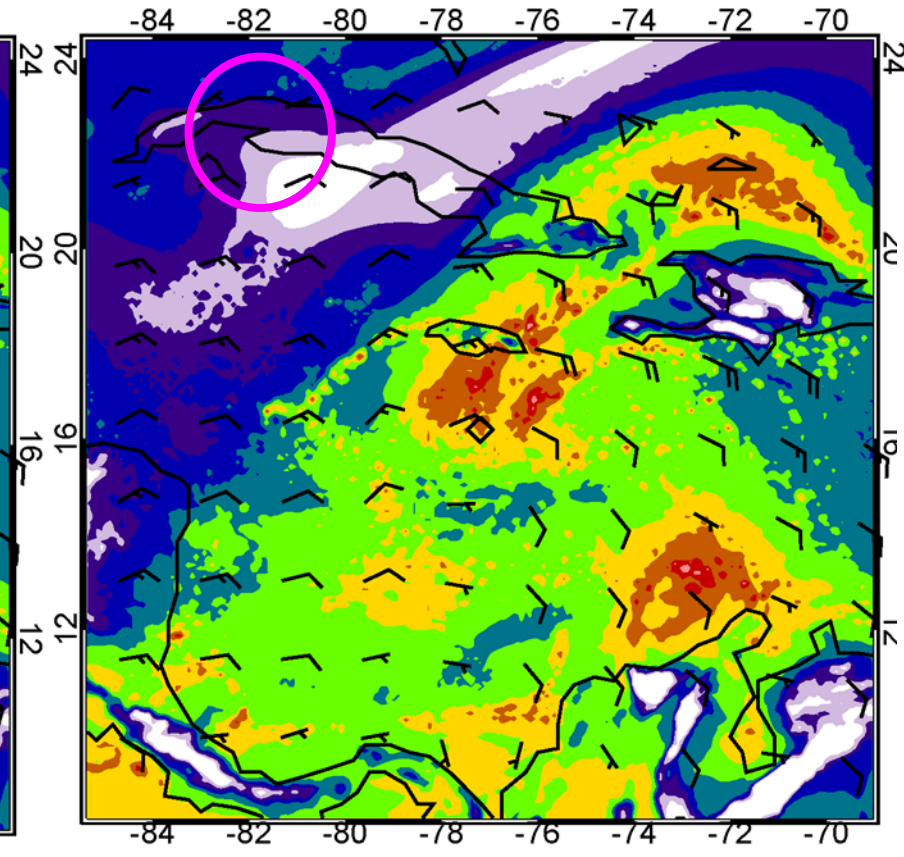
GDAEc

GDAEc_sfc TPW,12Z 13/09/2010



GDAEd

GDAEd TPW,12Z 13/09/2010



TPW(mm)

80

70

60

50

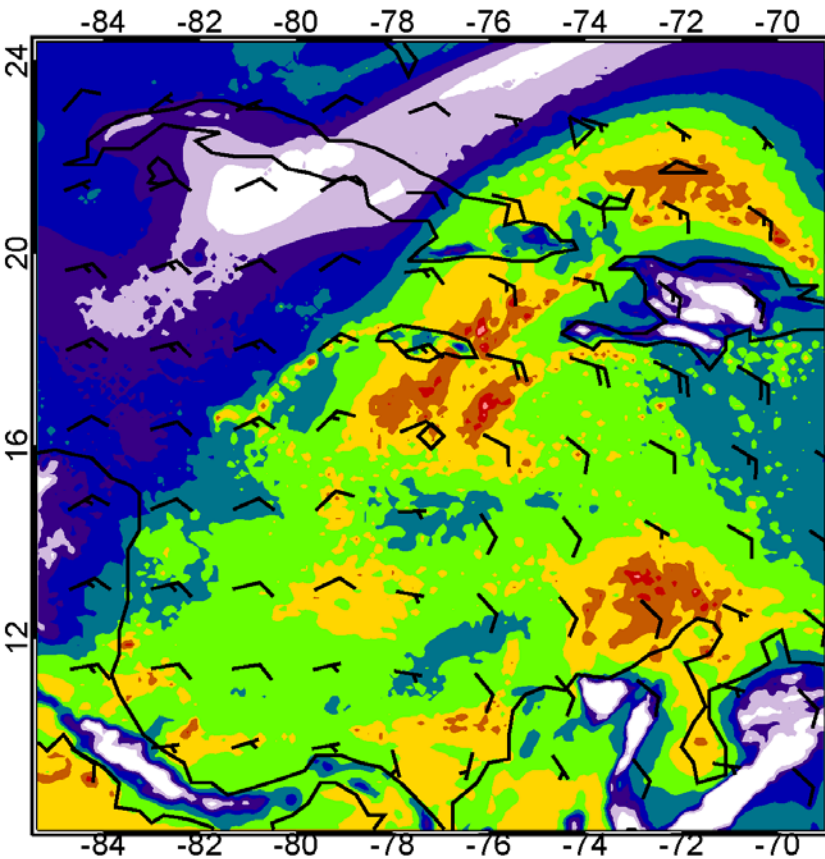
40

30

TPW Analysis (12Z 13 Sep.)

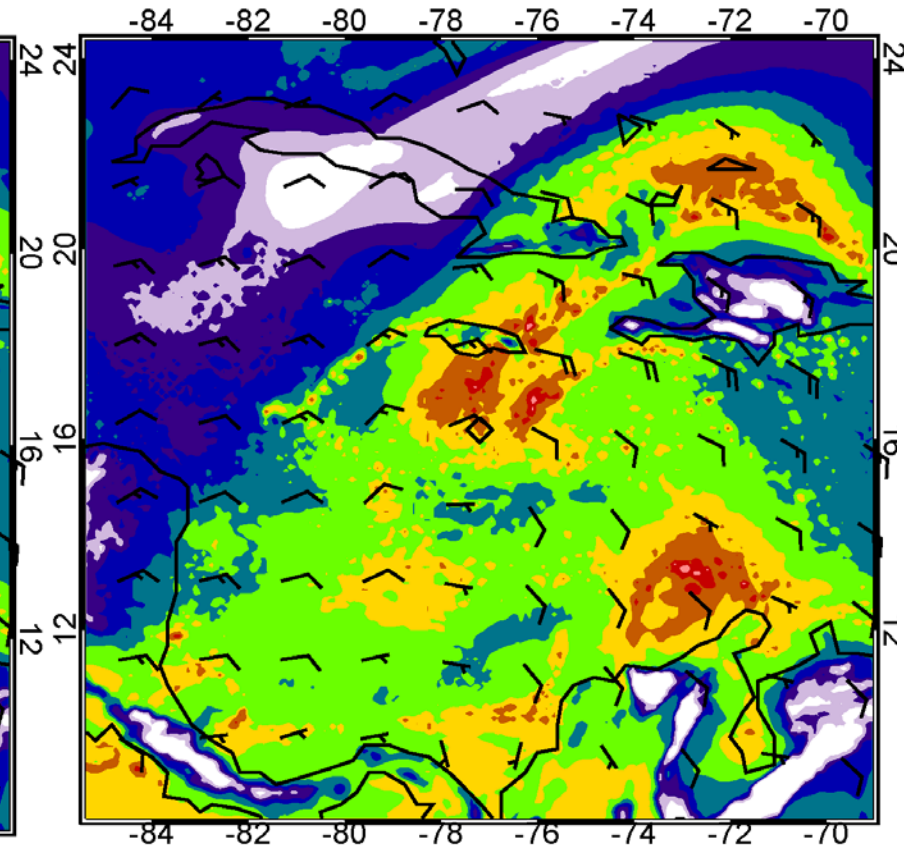
GDAEc

GDAEc_sfc TPW,12Z 13/09/2010



GDAEd

GDAEd TPW,12Z 13/09/2010



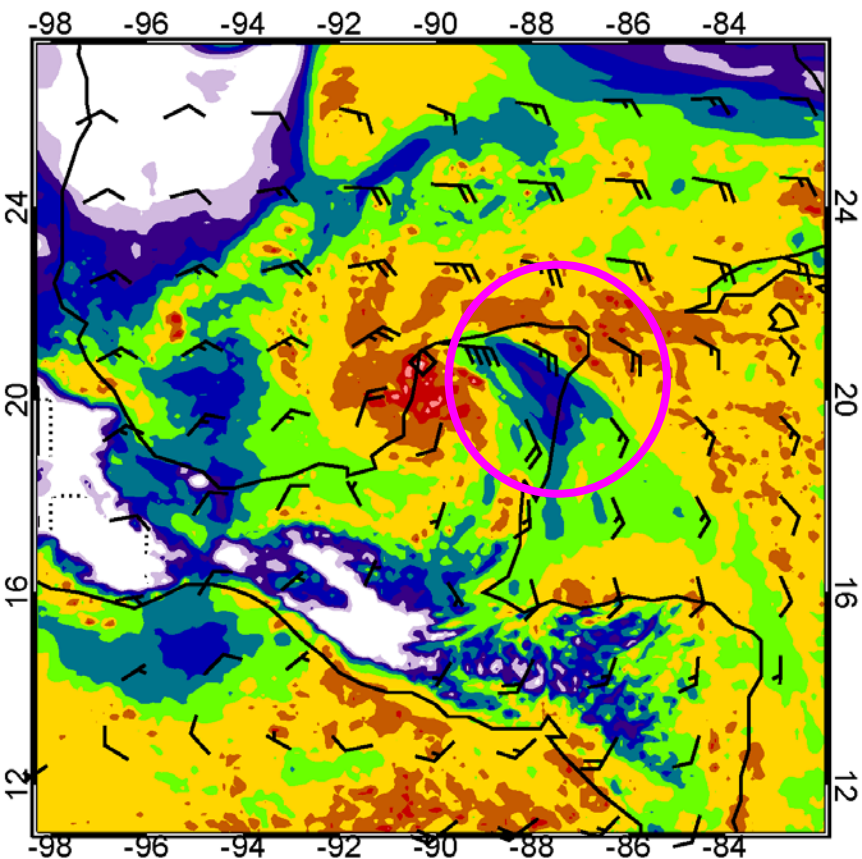
TPW(mm)



TPW (00Z 16 Sep)

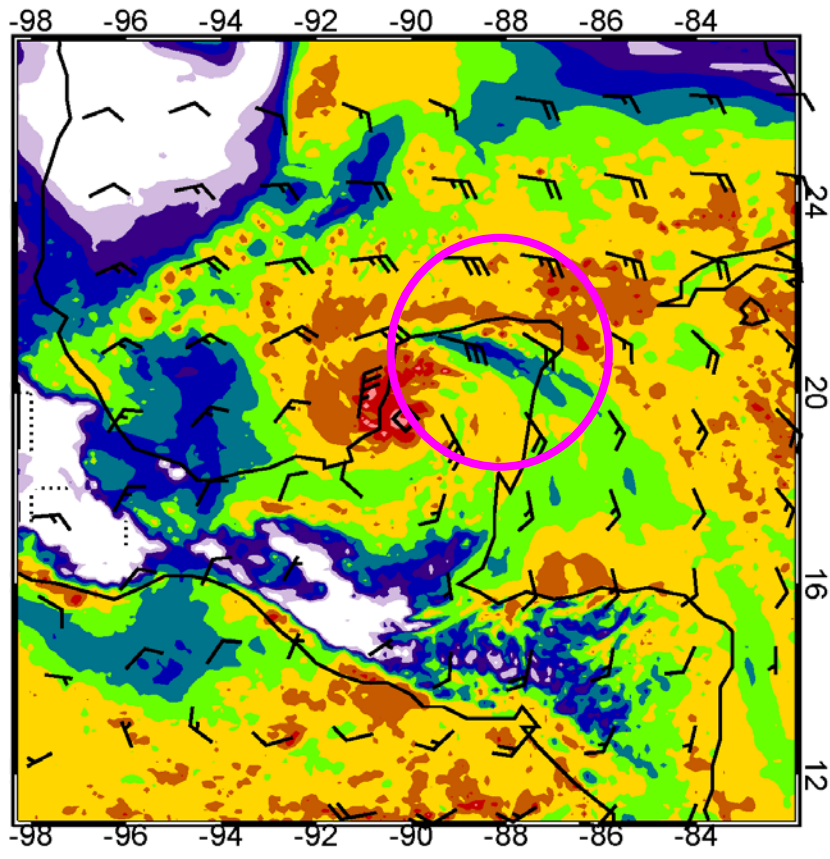
GDAEc

GDAEc_sfc TPW,00Z 16/09/2010

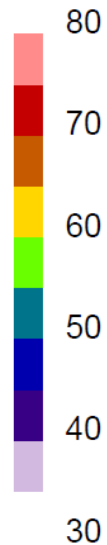


GDAEd

GDAEd TPW,00Z 16/09/2010



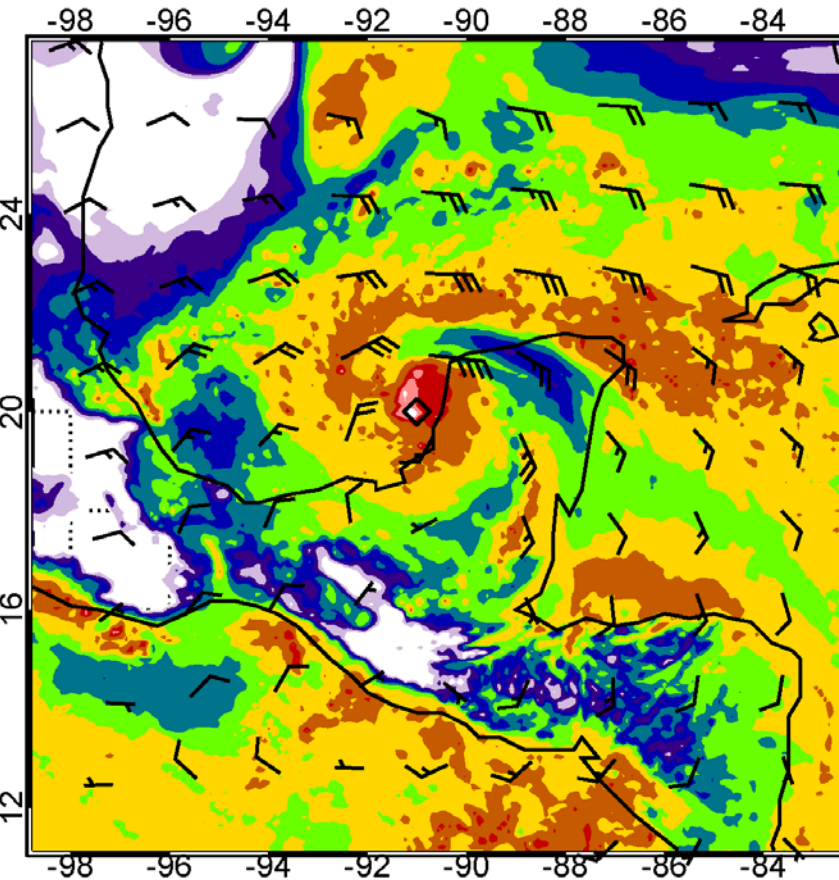
TPW(mm)



TPW (03Z 16 Sep)

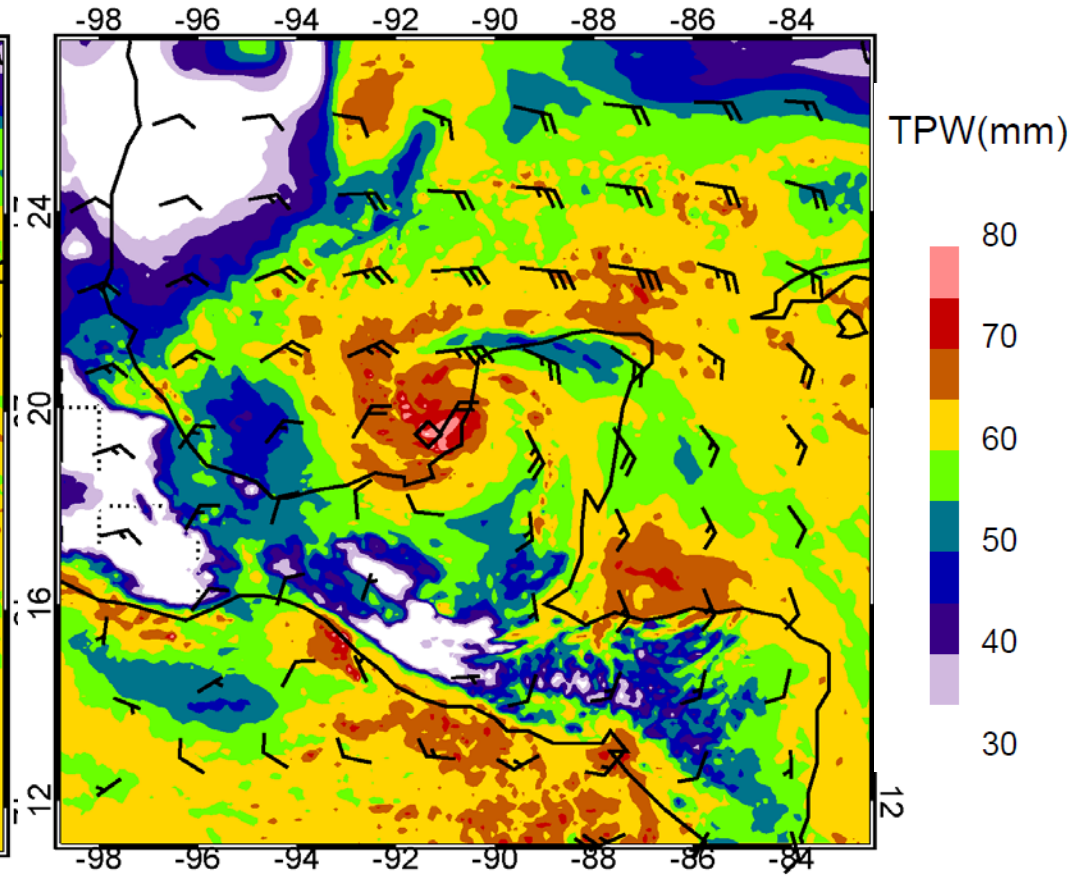
GDAEc

GDAEc_sfc TPW,03Z 16/09/2010



GDAEd

GDAEd TPW,03Z 16/09/2010

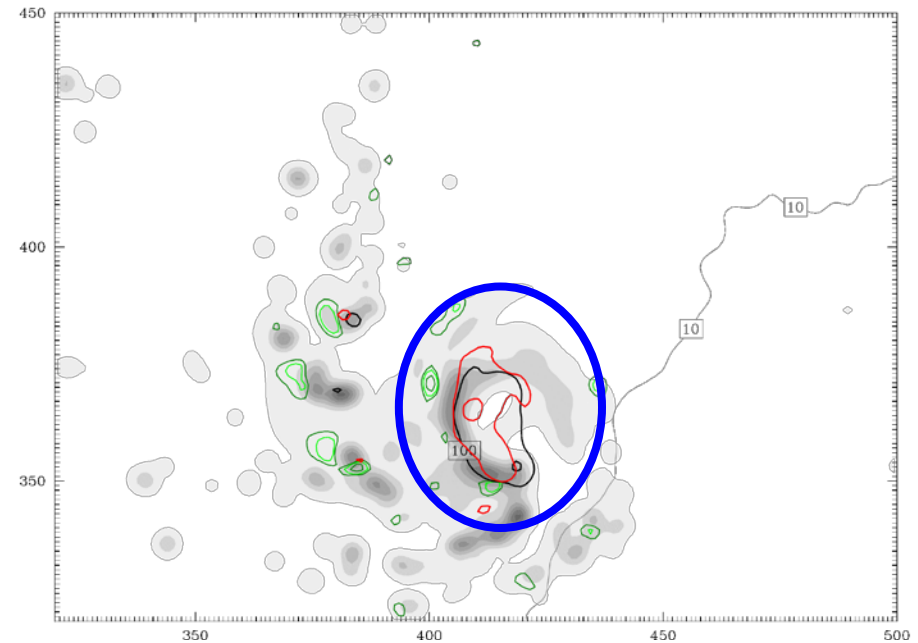


Diabatic Cooling (Color Contours)

GDAEc

06Z Sep 16, 850 mb

GDAEd



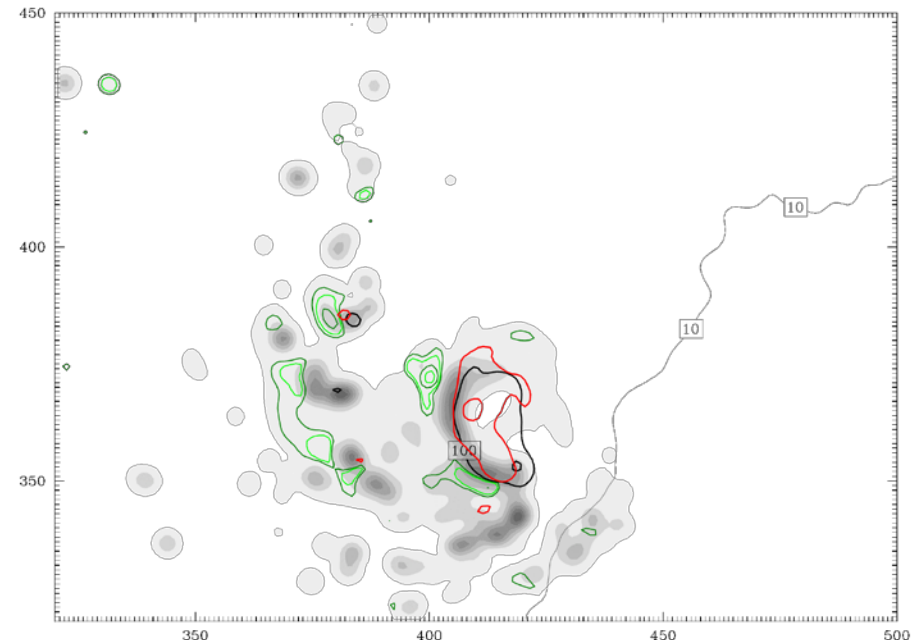
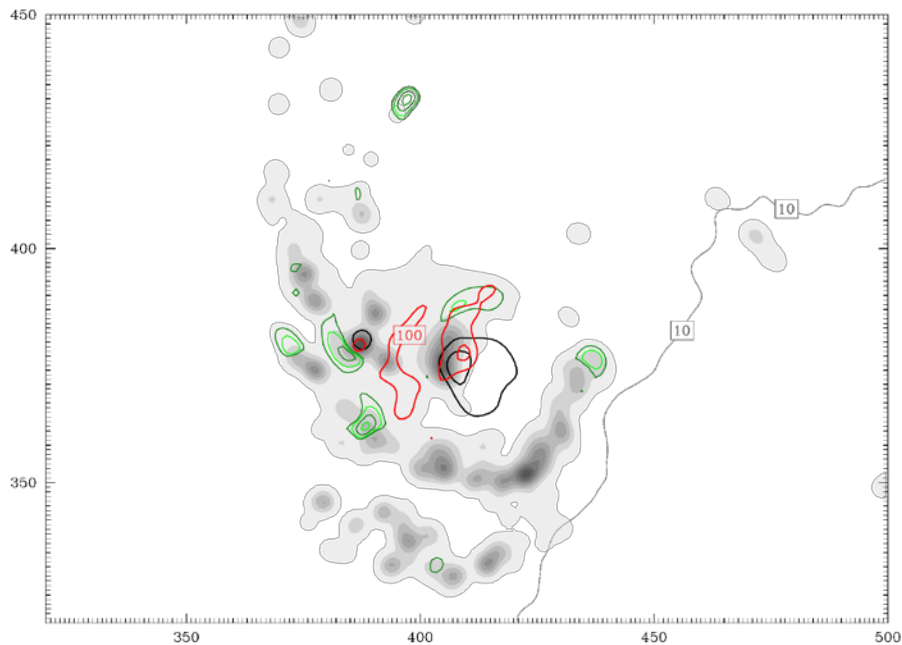
— 850 mb relative vorticity
— 500 mb relative vorticity

Diabatic Cooling (Color Contours)

GDAEc

06Z Sep 16, 800 mb

GDAEd



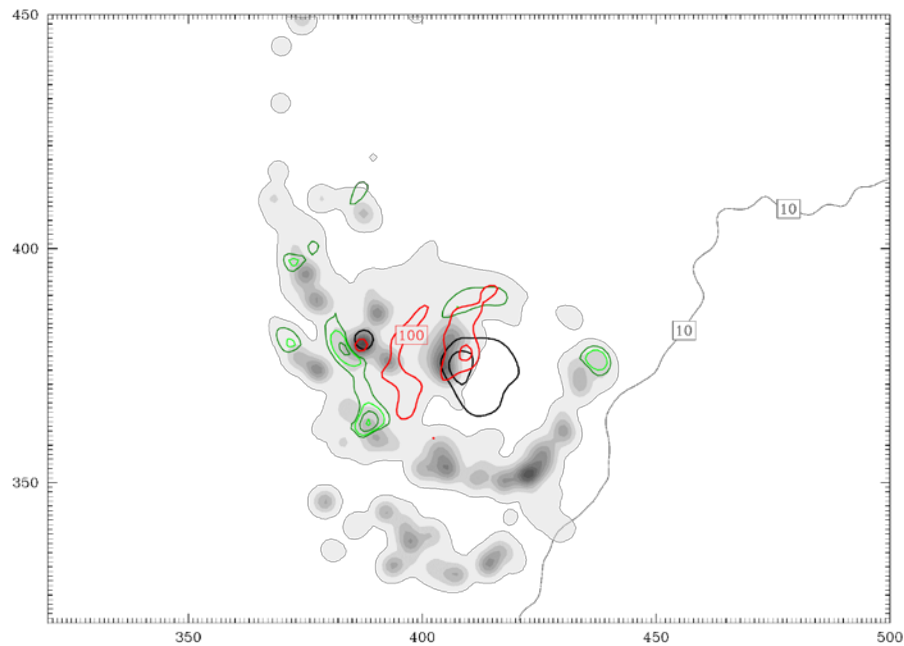
850 mb relative vorticity
500 mb relative vorticity

Diabatic Cooling (Color Contours)

GDAEc

06Z Sep 16, 750 mb

GDAEd



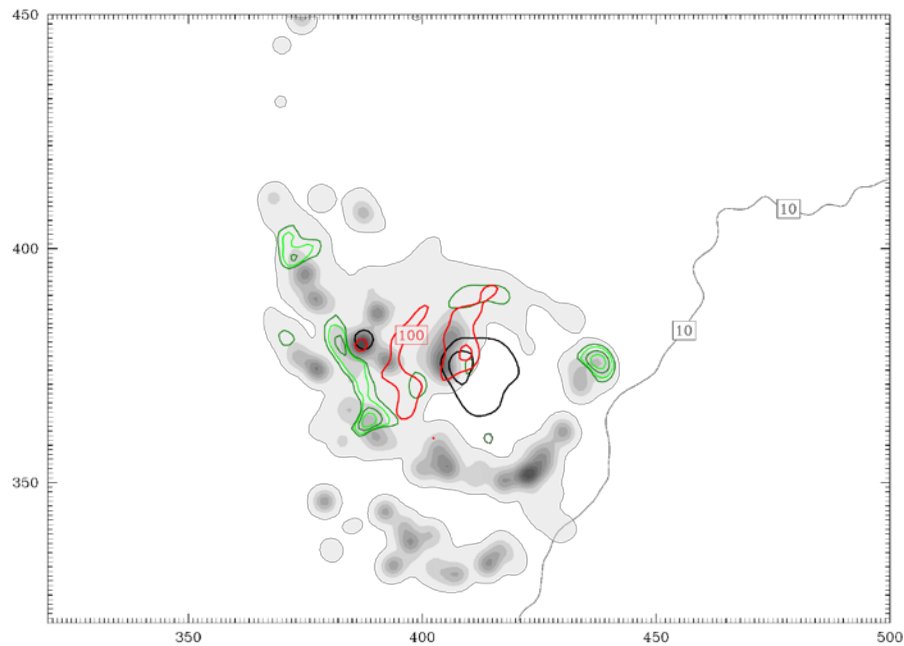
————— 850 mb relative vorticity
————— 500 mb relative vorticity

Diabatic Cooling (Color Contours)

GDAEc

06Z Sep 16, 700 mb

GDAEd



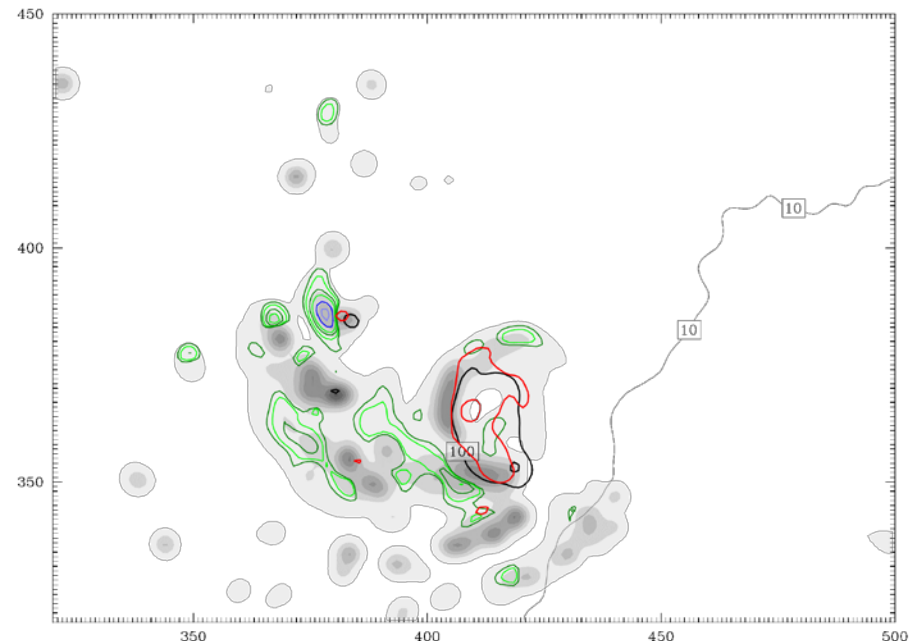
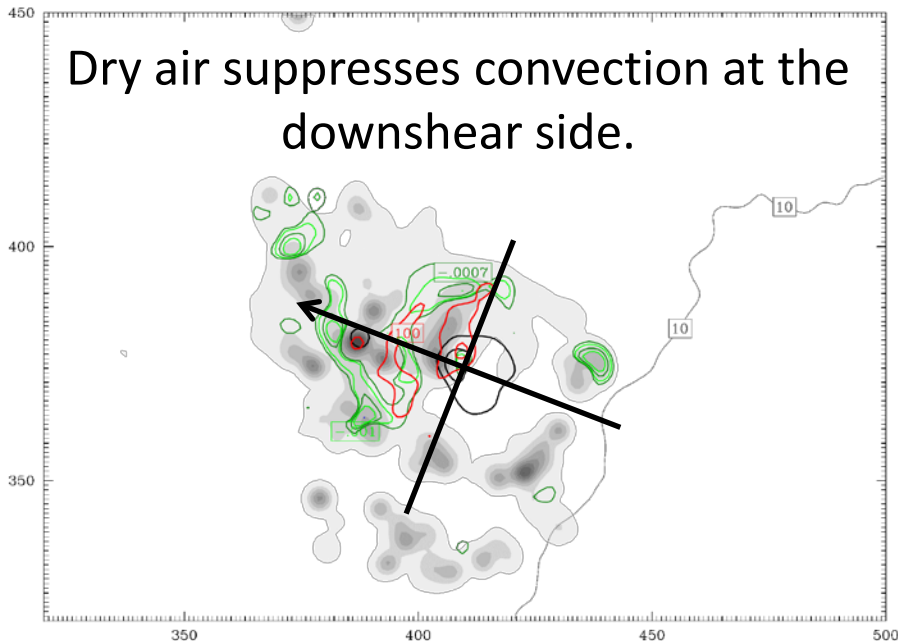
— 850 mb relative vorticity
— 500 mb relative vorticity

Diabatic Cooling (Color Contours)

GDAEc

06Z Sep 16, 600 mb

GDAEd



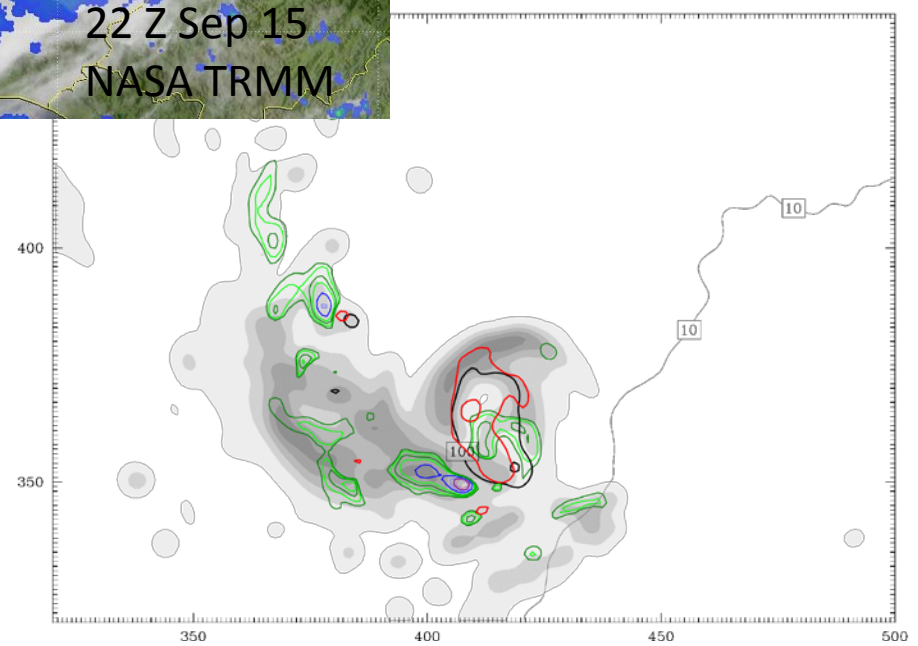
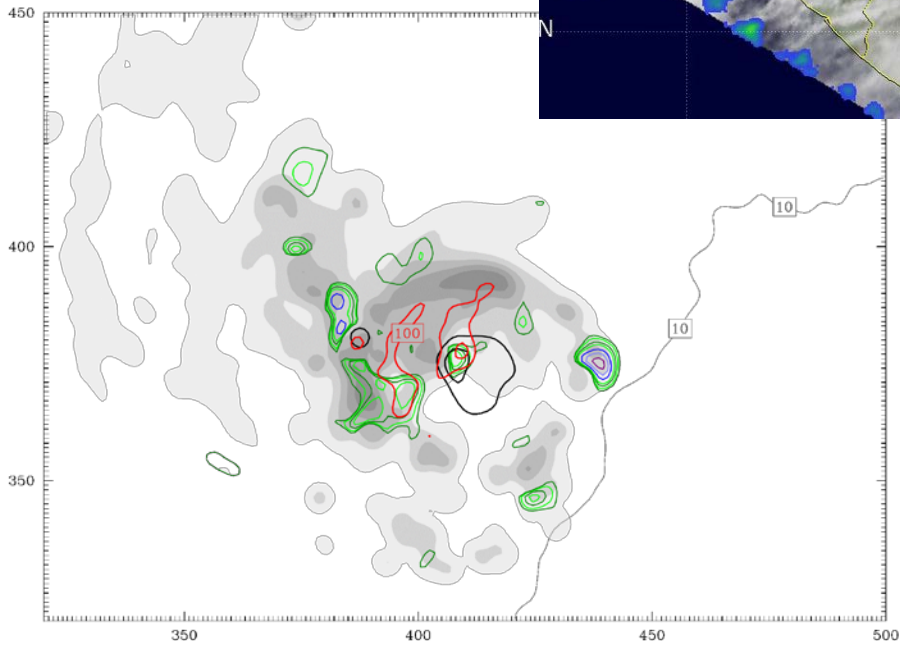
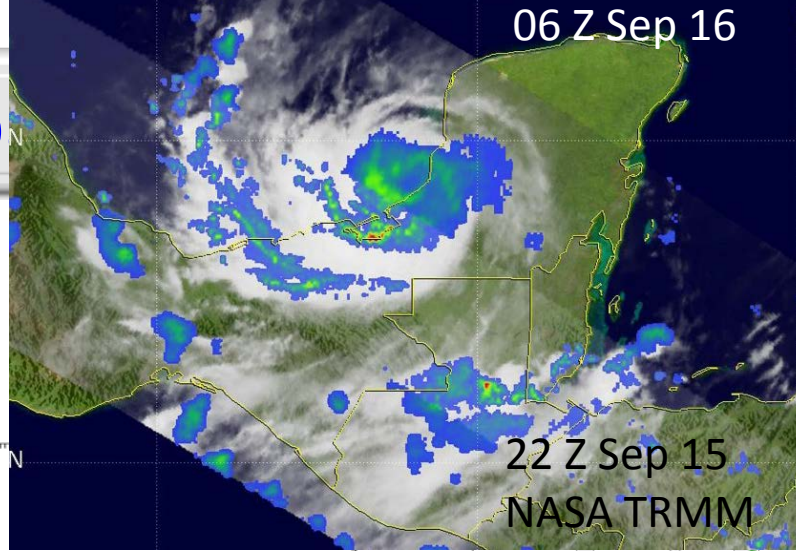
Observations show that the presence of more convective bursts on the downshear side of the storms within R_{MW} is one of the distinct indicators of an intensifying cyclone. (Roger et al. 2013)

Diab

(hours)

GDAEc

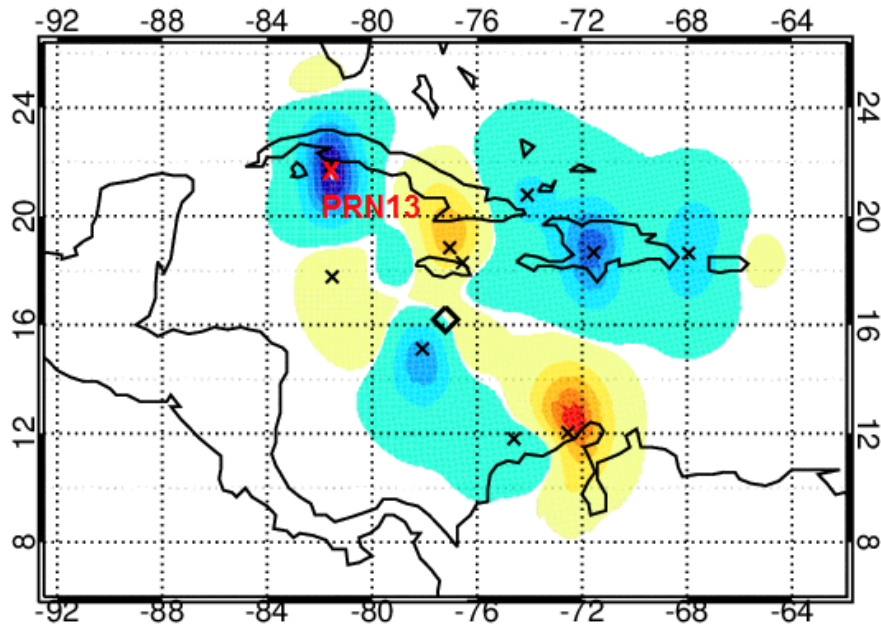
GDAEd



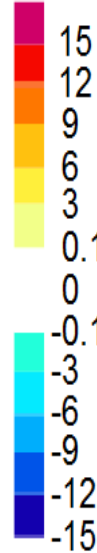
— 850 mb relative vorticity
— 500 mb relative vorticity

Drier Air and prn 13

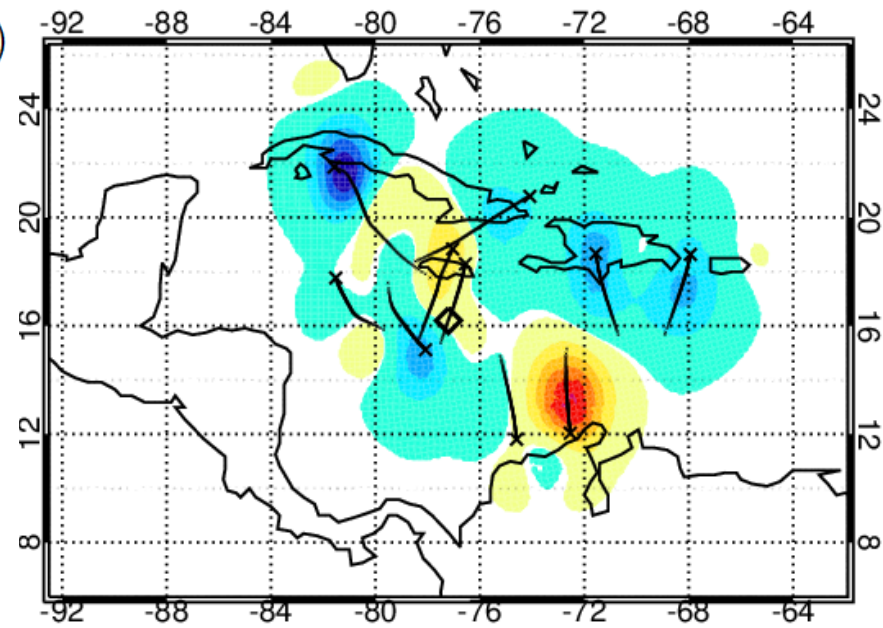
GDAEc – CTRL



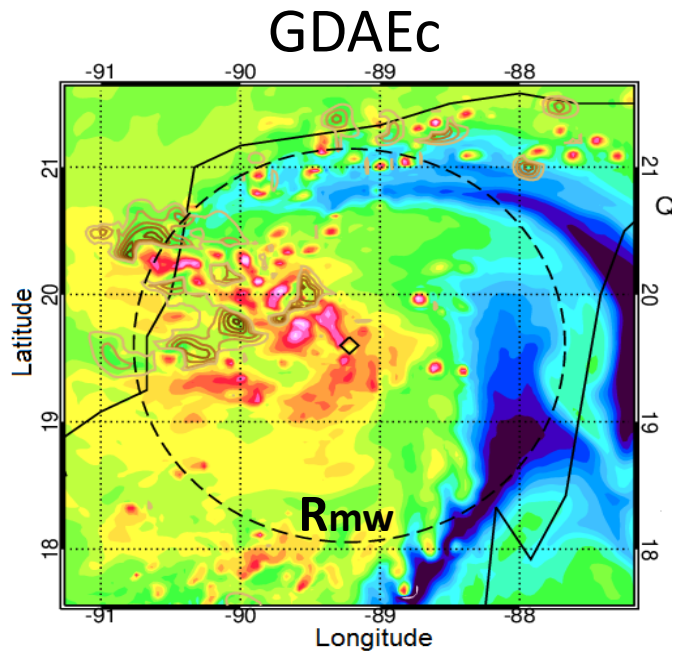
TPW (%)



GDAEd – CTRL

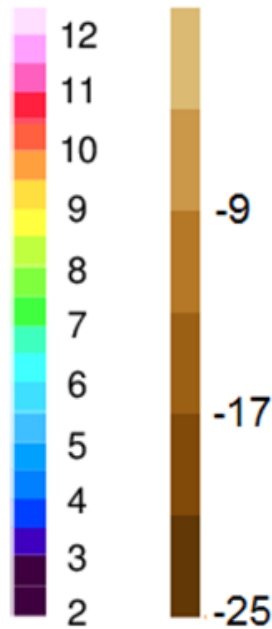


Diabatic Cooling @ 650 mb (Color Contours)

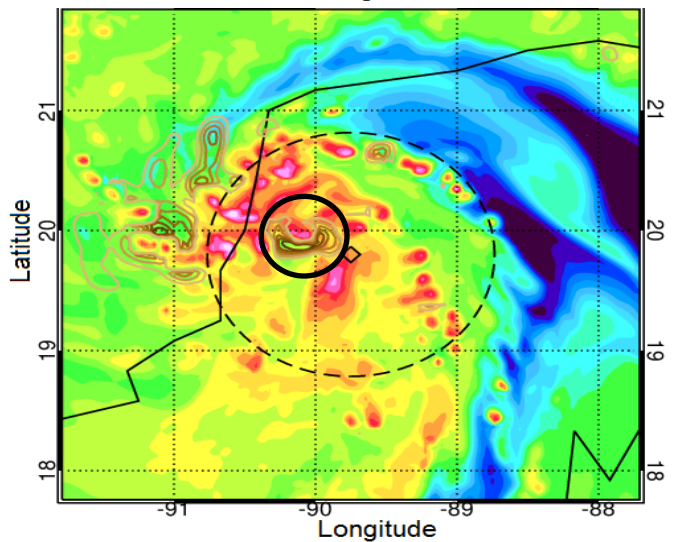


21Z 15 Sep

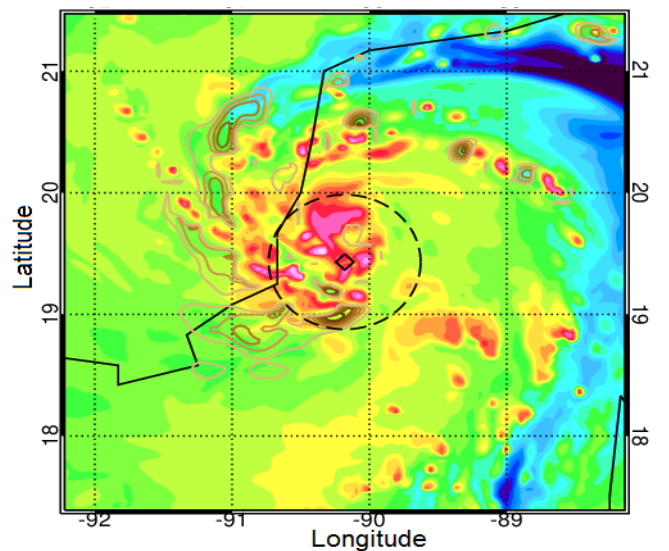
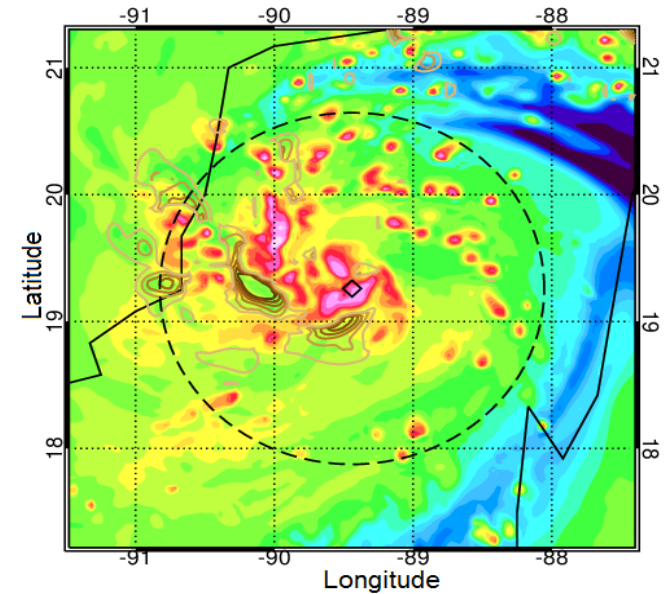
Diab. H
QV(g/kg) (10^{-4} K/s)



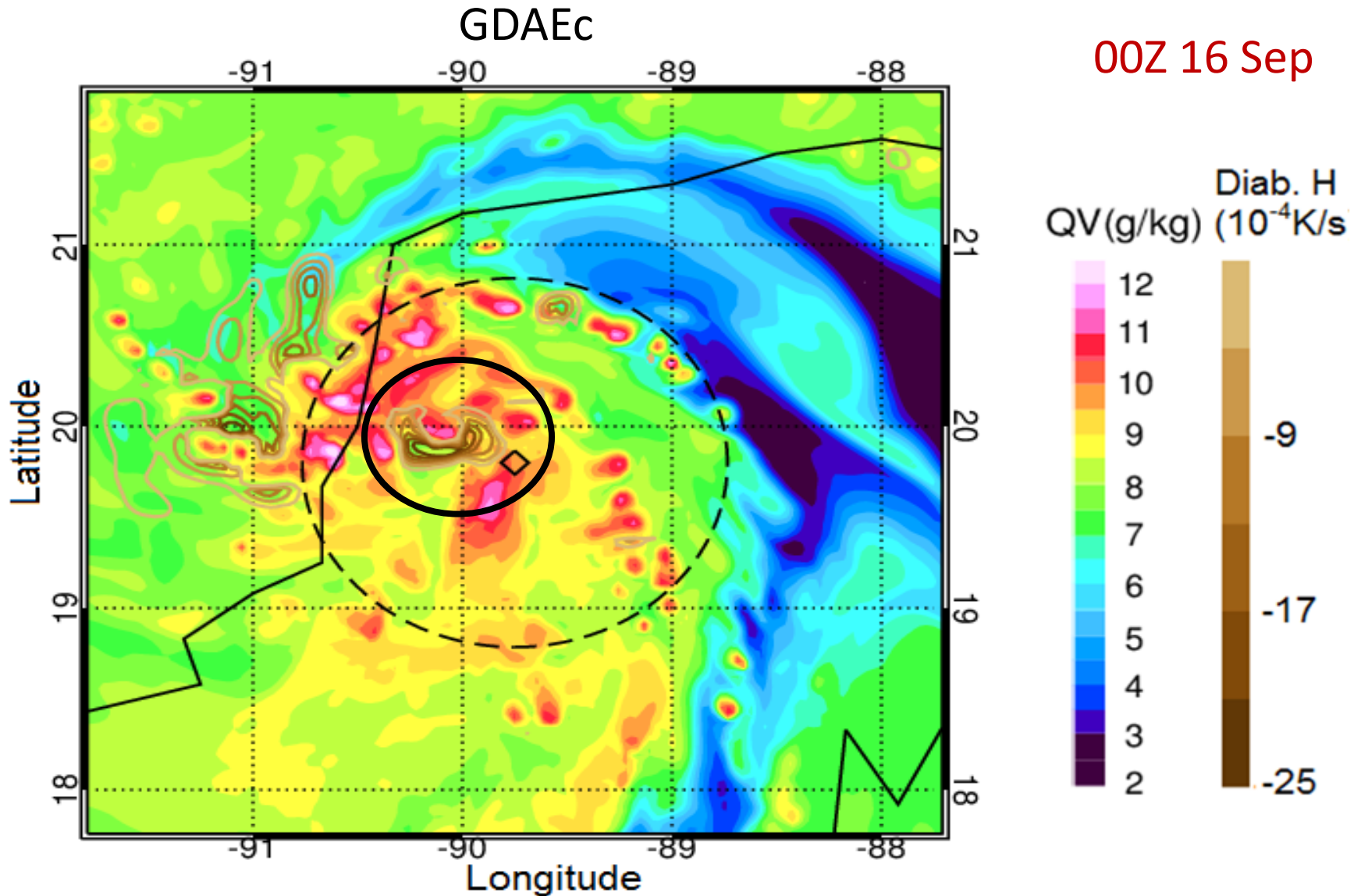
00Z 16 Sep



GDAEd

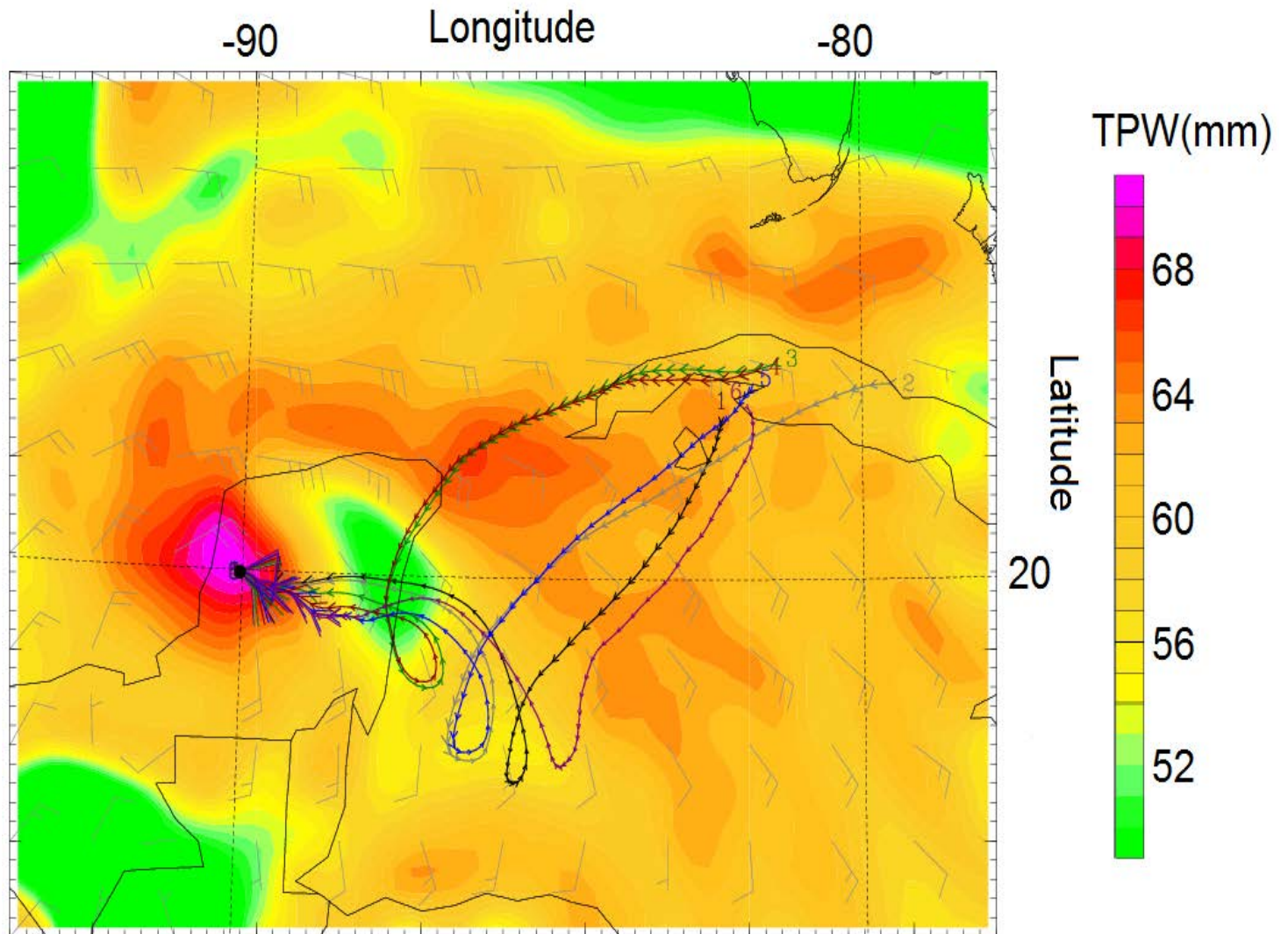


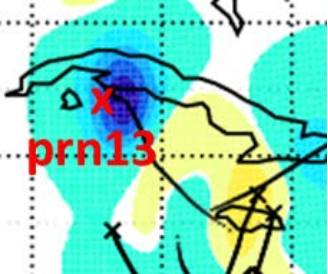
Diabatic Cooling @ 650 mb (Color Contours)



Backward Trajectory (GDAEc)

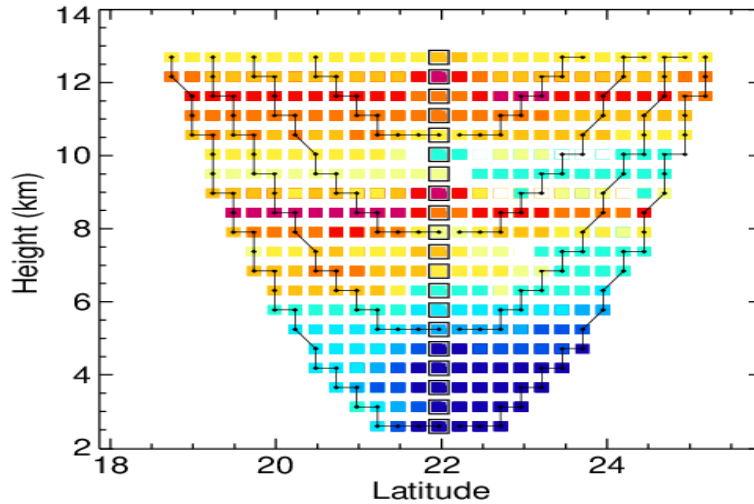
00Z 16 to 12Z 13 Sep



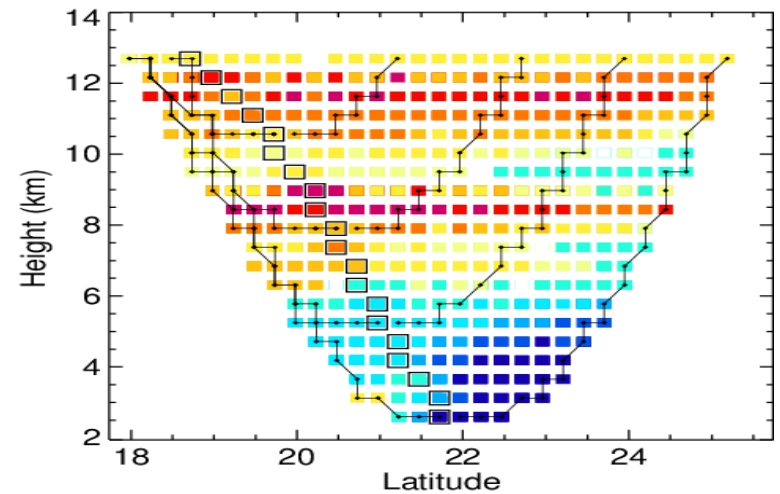


Innovations & Increments (prn 13)

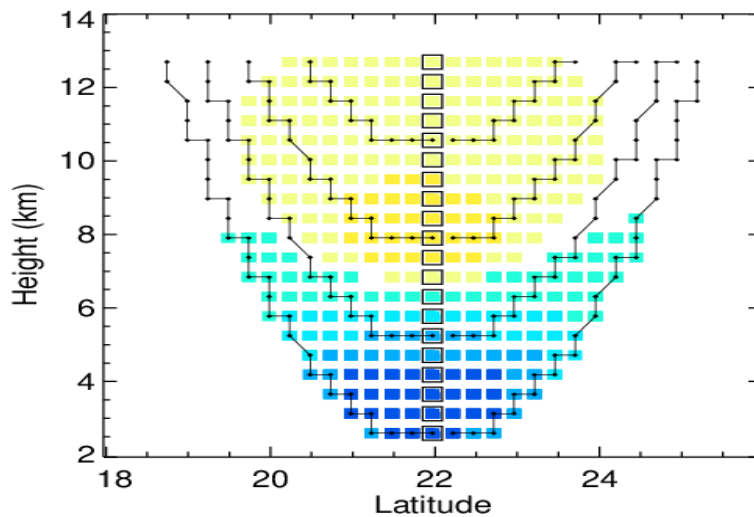
GDAEc innovation



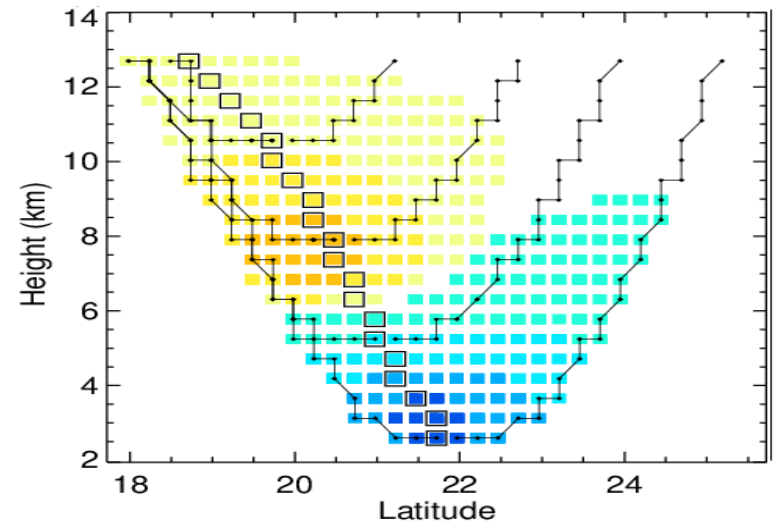
GDAEd innovation



GDAEc increment

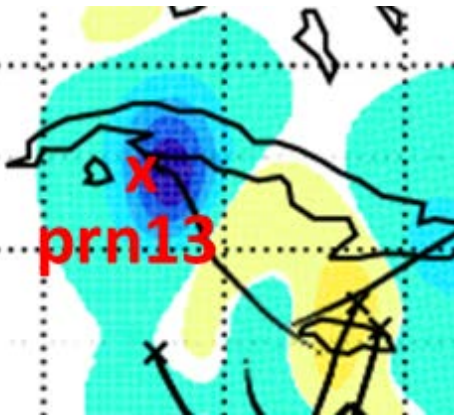
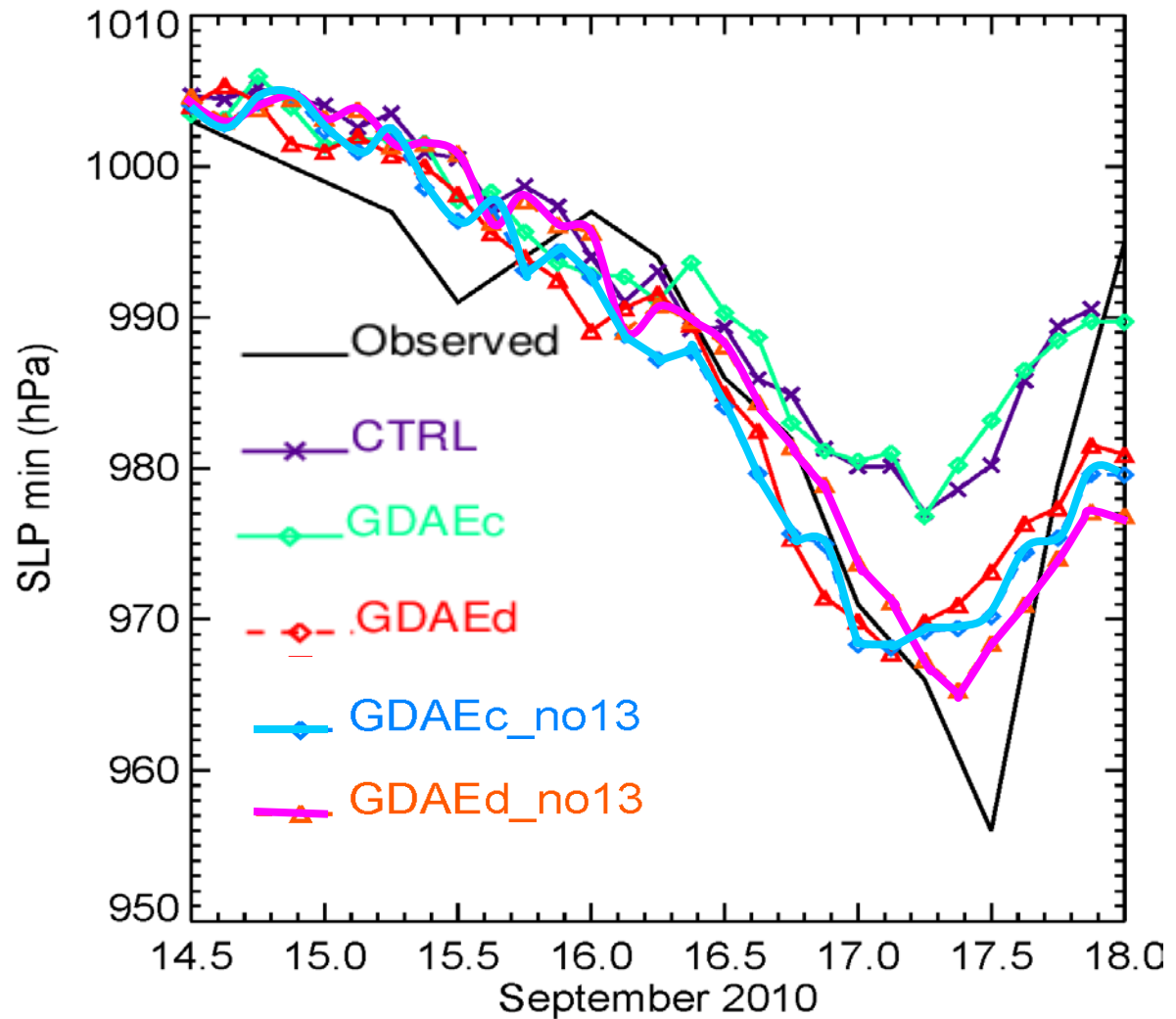


GDAEd increment



Sensitivity Experiments – Remove prn 13

Min SLP, 12Z 14 Sep – 00Z 18 Sep 2010



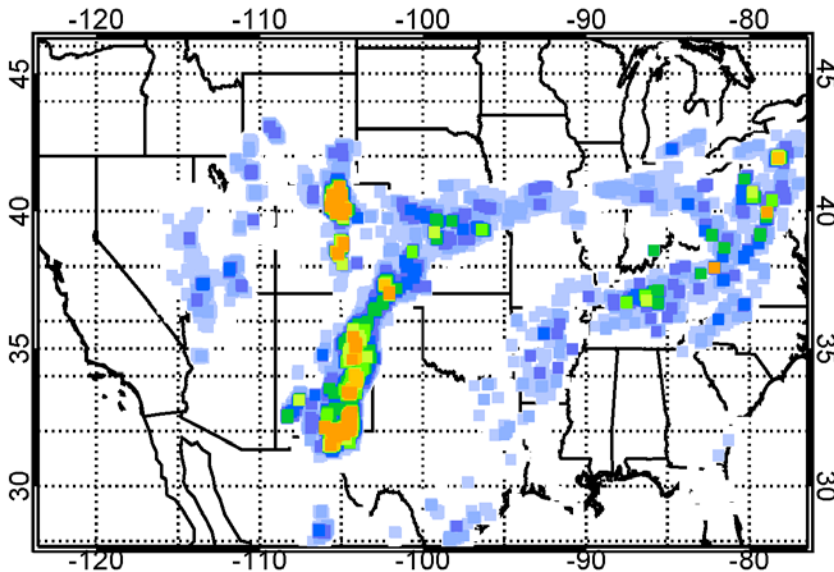
Summary

- **ARO data has potential to improve severe weather forecasts.**
- **Assimilating AROs with drifting tangent points gave better results than without drifting. (Drier air intruded into the middle levels of the downshear side of the storm.)**
- **Although in this case study the non-local RO data did not give a better result than the local RO data, the non-local operator should be still preferred.**
- **How can EnKF methods better take the advantage of the information given by non-local observations, which have smaller errors?**

Ongoing Work

- Repeat the case study using a LETKF system.
- Conduct an OSSE study: Colorado Floods in Sep 2013

NWS obs. 24hr precip.(mm) ending on 2013-09-12 12Z



NR accum.rain 11 12UTC-12 12UTC and trajs @ 00UTC+/-3 10/09/2013

